

# Carrier Dynamics of Polar, Semipolar, and Nonpolar InGaN/GaN LEDs Measured by Small-Signal Electroluminescence

Prof. Daniel Feezell

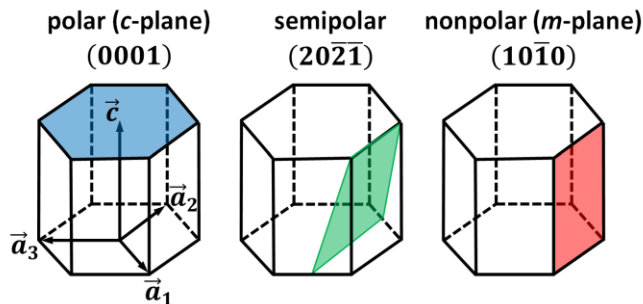
X. Li<sup>1</sup>, E. DeJong<sup>1</sup>, N. Pant<sup>2</sup>, M. Monavarian<sup>1</sup>, A. Rashidi<sup>1</sup>, M. Nami<sup>1</sup>, A. Rishinaramangalam<sup>1</sup>, A. Armstrong<sup>3</sup>, E. Kioupakis<sup>2</sup>, and R. Armitage<sup>4</sup>

<sup>1</sup>*Center for High Technology Materials, University of New Mexico, Albuquerque, NM, USA*

<sup>2</sup>*Department of Materials Science & Engineering, University of Michigan, Ann Arbor, MI, USA*

<sup>3</sup>*Sandia National Laboratories, Albuquerque, NM, USA*

<sup>4</sup>*Lumileds LLC, San Jose, CA, USA*



# Outline

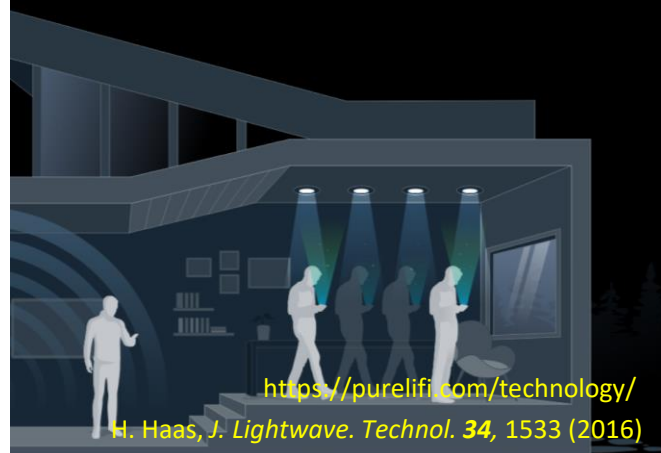
---

- Carrier dynamics measurements and modeling with small-signal EL
- *c*-Plane wavelength series on commercial epitaxy
- *c*-Plane growth quality (defect density) series on commercial epitaxy
- Crystal orientation series
- Core-shell nanostructure-based LEDs

# Motivation for Carrier Dynamics/Modulation Studies



## Visible-Light Communication



<https://purelifi.com/technology/>

H. Haas, *J. Lightwave. Technol.* **34**, 1533 (2016)

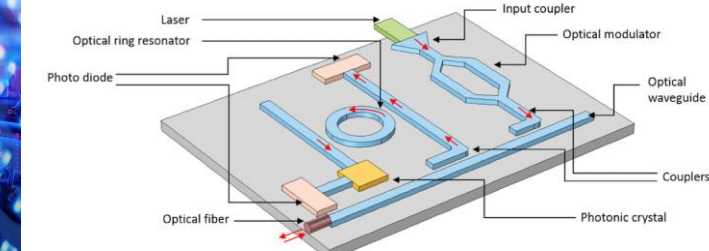
## Augmented and Virtual Reality



## Micro-LED Displays

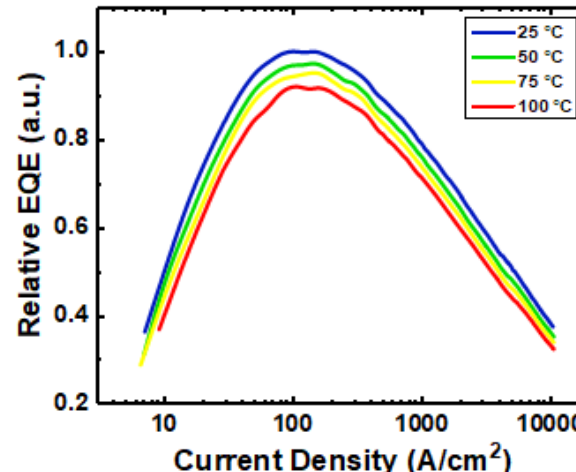


## Photonic Integration

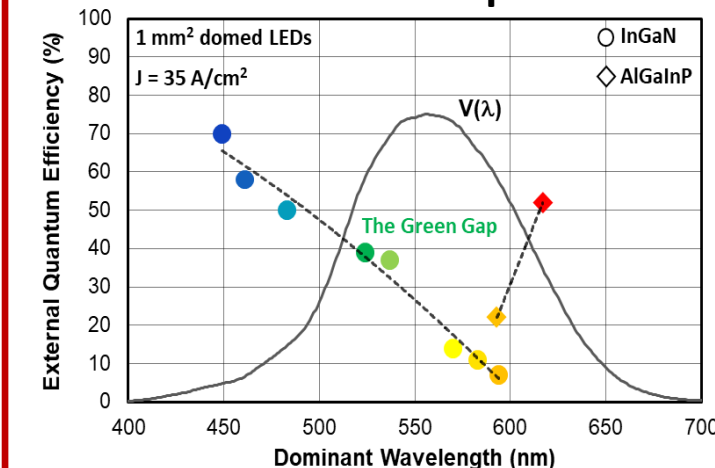


B.E.A. Saleh and M.C. Teich, *Fundamentals of Photonics*

## Efficiency/Thermal Droop

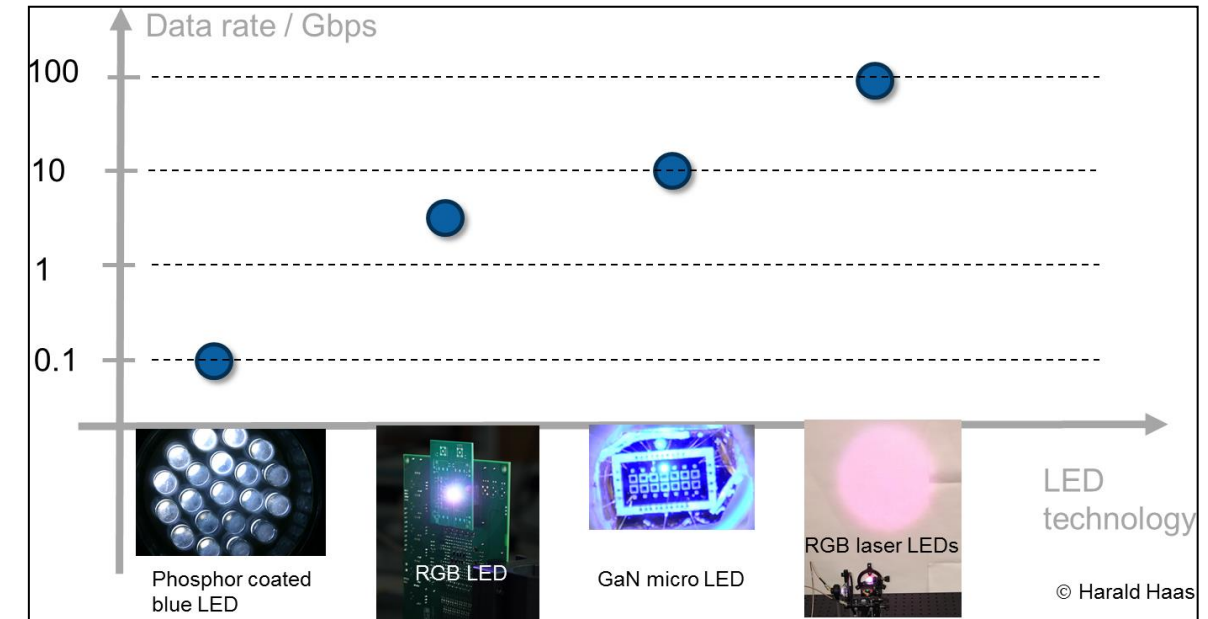
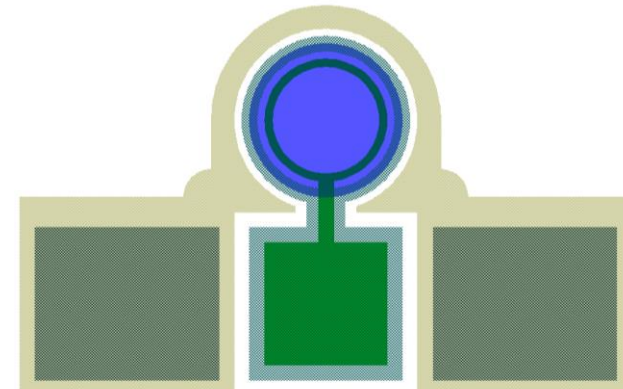
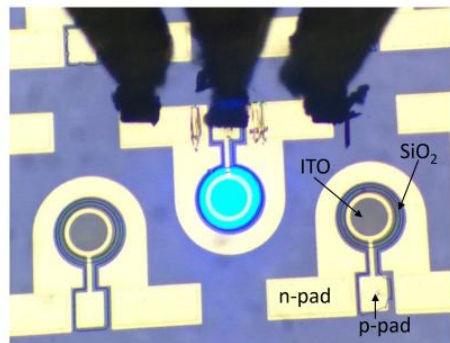
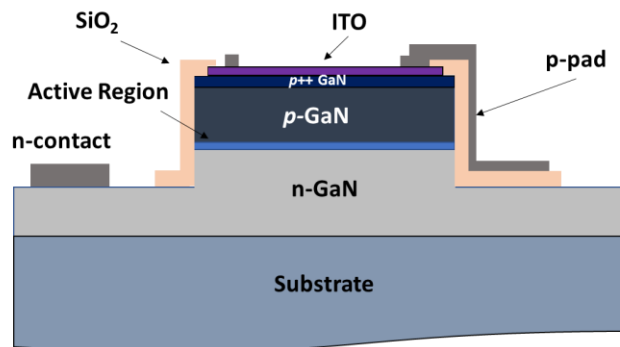


## Green Gap

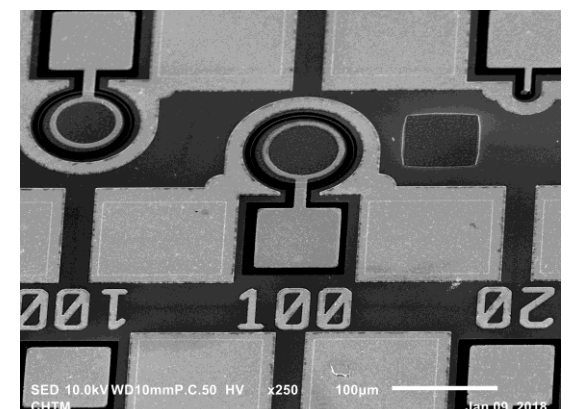
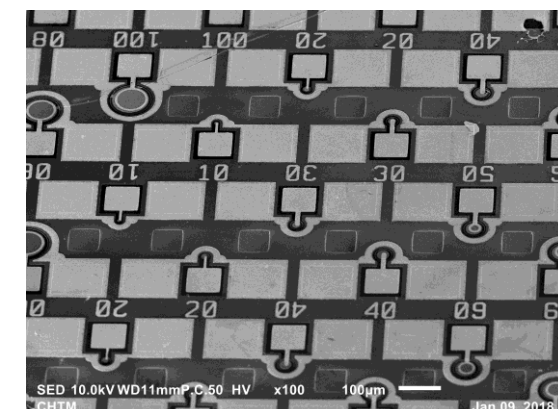


# Small-Area GaN-Based LEDs

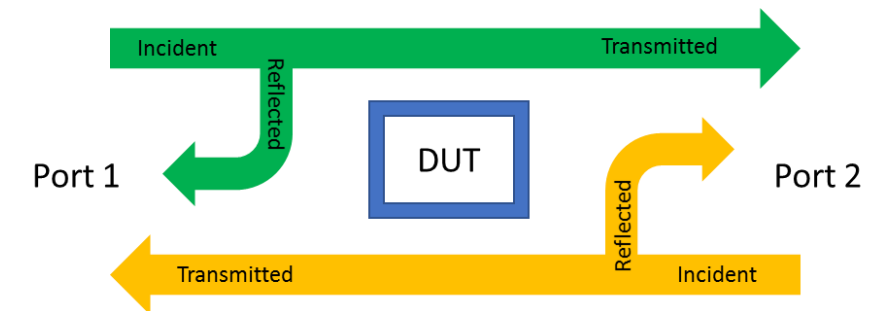
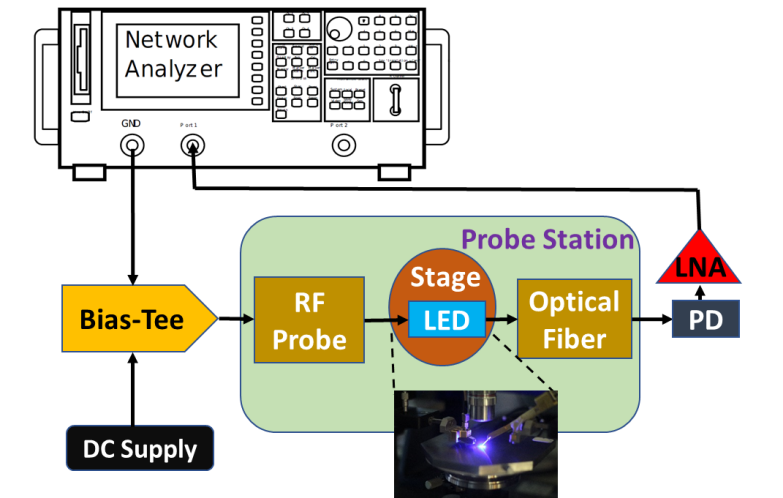
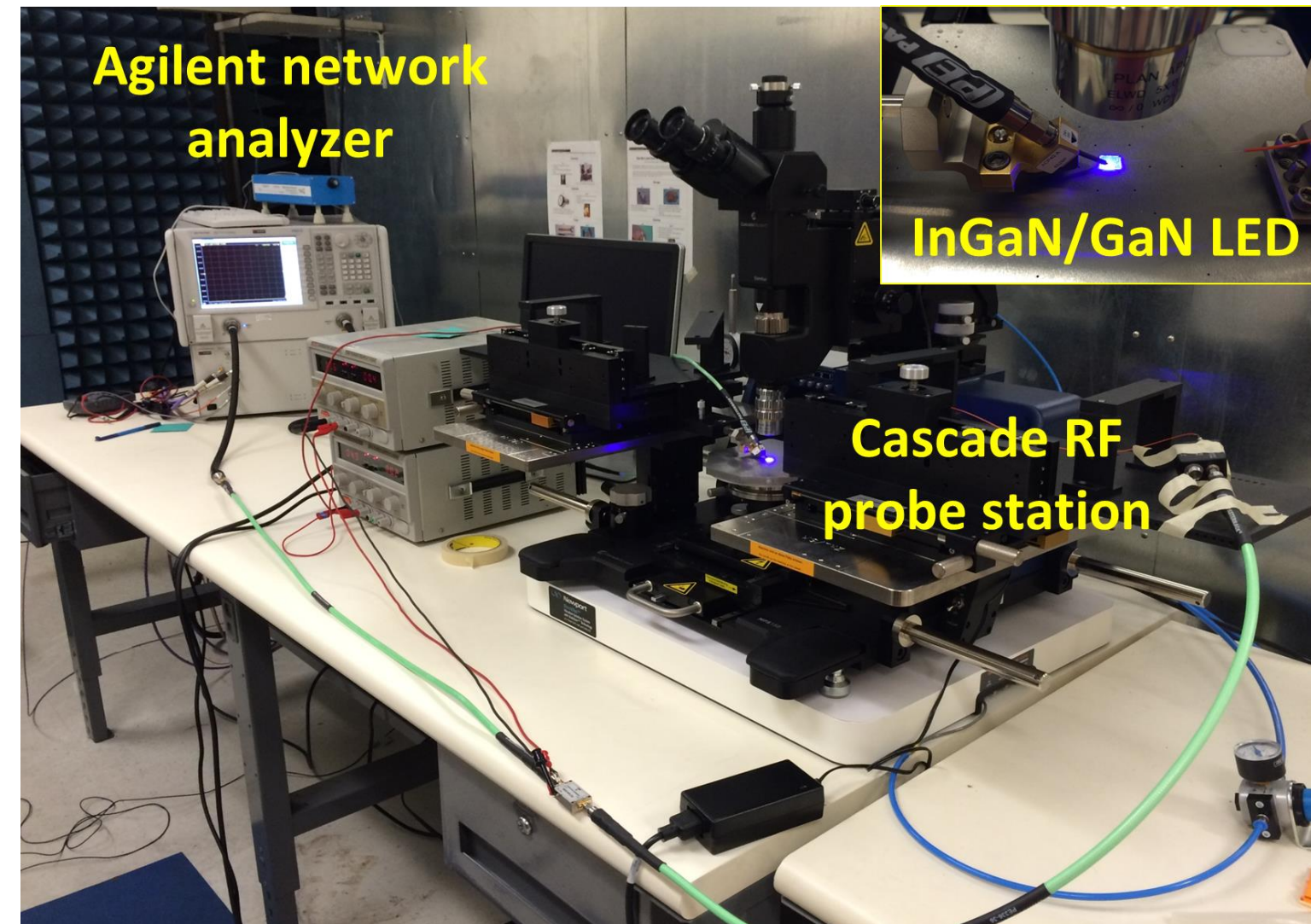
- Small area reduces RC parasitics
- 50 – 100  $\mu\text{m}$  diameter
- Can be driven at high current density



<https://www.lifi.eng.ed.ac.uk/lifi-news/2015-11-28-1320/how-fast-can-lifi-be>



# RF Measurement System



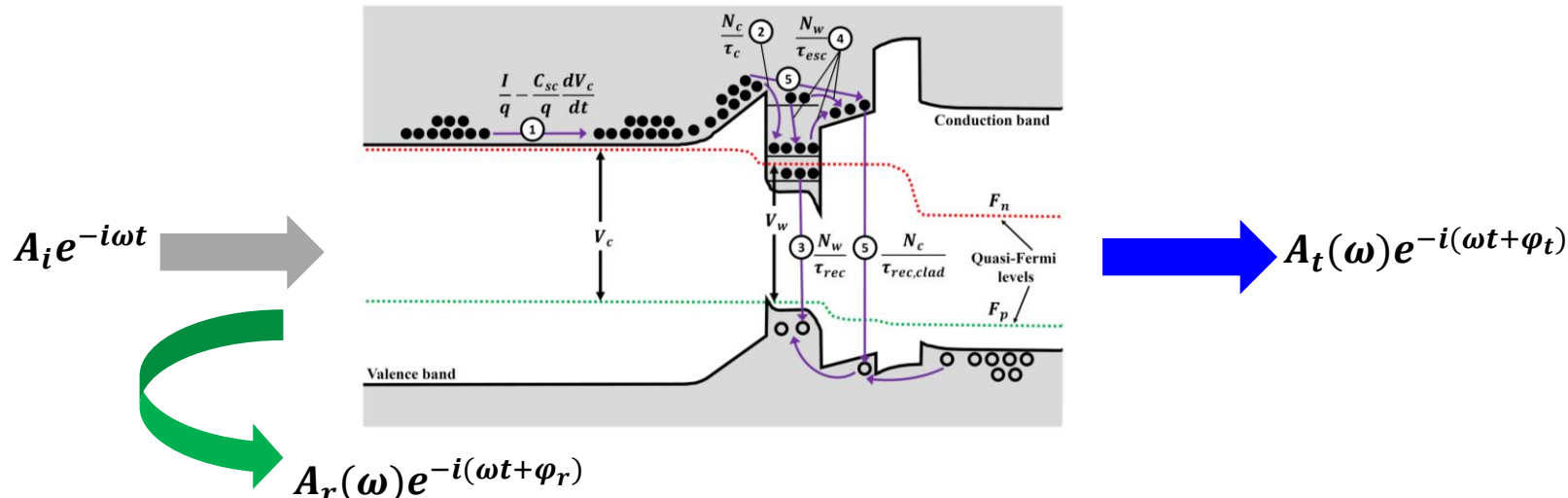
$$S_{11} = \frac{\text{Reflected}}{\text{Incident}}$$

$$S_{21} = \frac{\text{Transmitted}}{\text{Incident}}$$

$$\text{Impedance} = Z = Z_0 \frac{1+S_{11}}{1-S_{11}}$$

$$\text{Optical Response} = S_{21}$$

# Rate Equation Modeling of LED Carrier Dynamics



## Considered carrier processes:

1. Carrier injection
2. Carrier diffusion and capture
3. Recombination in QW
4. Carrier leakage
5. Recombination in cladding and overshoot

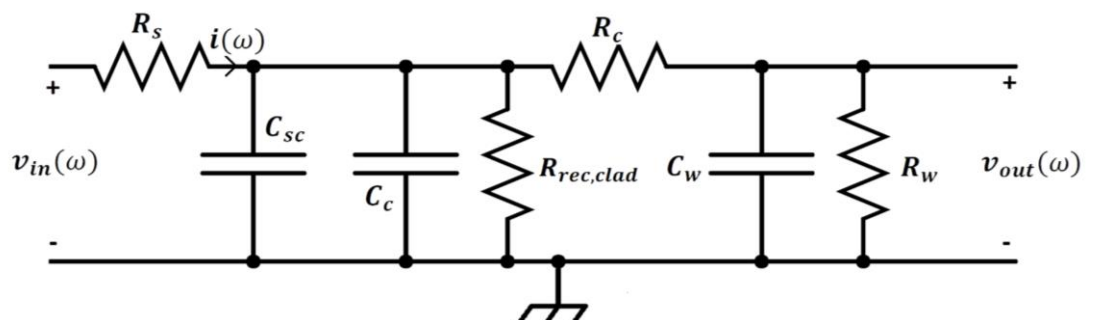
## Small-signal rate equations

$$j\omega n_w = - \left[ \frac{1}{\tau_{\Delta rec}} + \frac{1}{\tau_{\Delta esc}} \right] n_w + \frac{n_c}{\tau_{\Delta c}}$$

$$j\omega n_c = \frac{i}{q} - j\omega v_c \frac{C_{sc}}{q} + \frac{n_w}{\tau_{\Delta esc}} - \frac{n_c}{\tau_{\Delta c}} - \frac{n_c}{\tau_{\Delta rec,clad}}$$



## Small-signal equivalent circuit



## Associated lifetimes

$$\tau_{\Delta rec} = R_w C_w \quad \tau_{\Delta RC} = \frac{R_s}{R_s + R_c} \tau_{\Delta 0}$$

$$\tau_{\Delta esc} = R_c C_w \quad \tau_{\Delta 0} = R_c C_{tot}$$

# Fitting Equivalent Circuit Model

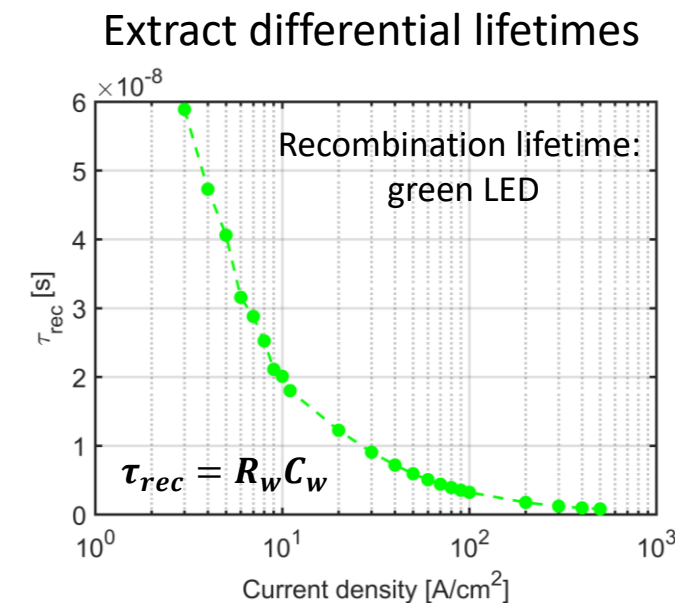
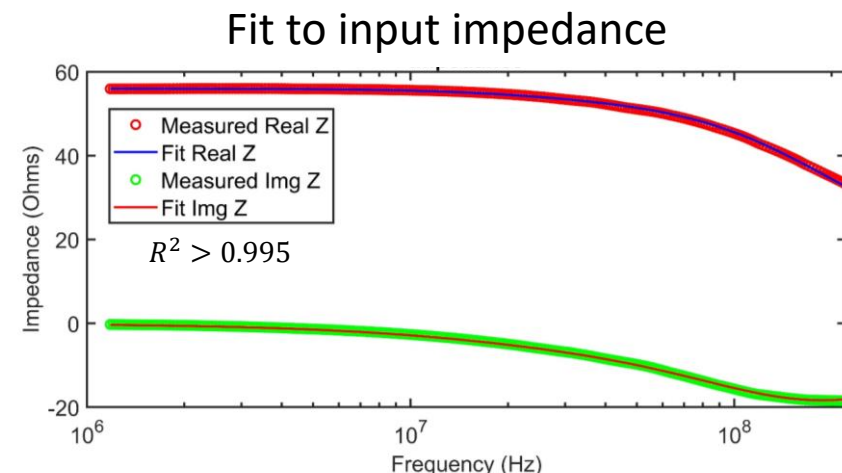
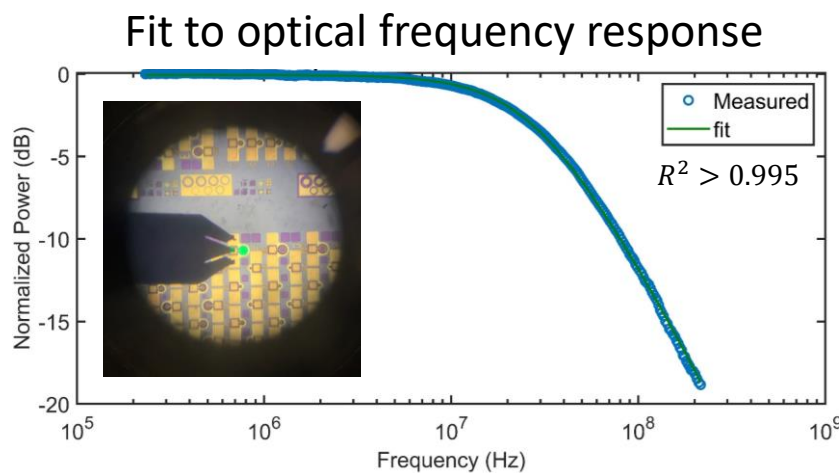
Simultaneous fitting of optical frequency response and impedance yields various carrier lifetimes

Optical response:

$$\frac{v_{out}}{v_{in}} = \frac{R_w}{R_s(1 + j\omega\tau_{rec})(1 + j\omega\tau_0) + R_s(j\omega R_w C_{tot}) + R_c(1 + j\omega\tau_{rec}) + R_w}$$

Input impedance:

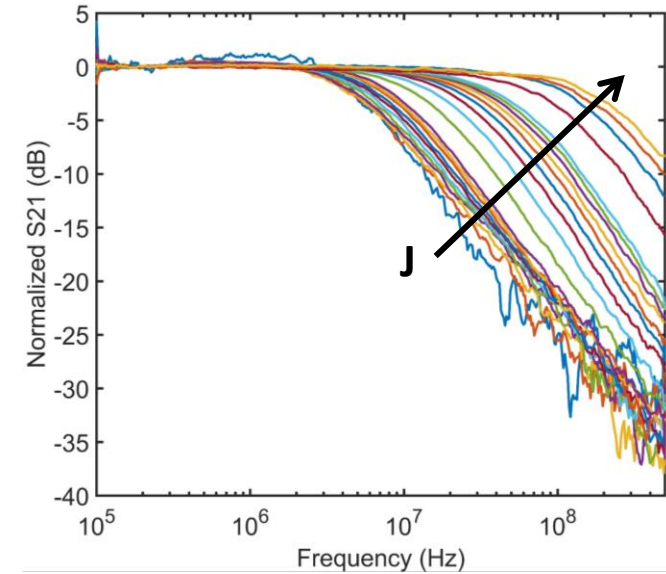
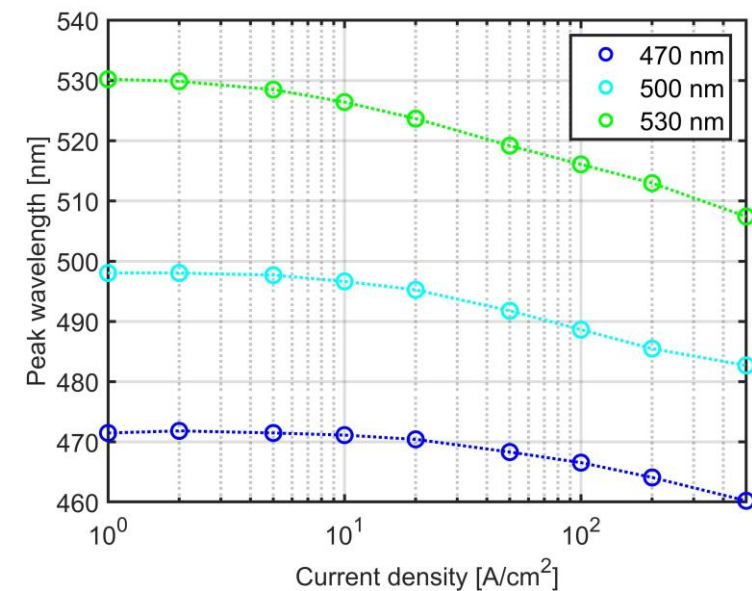
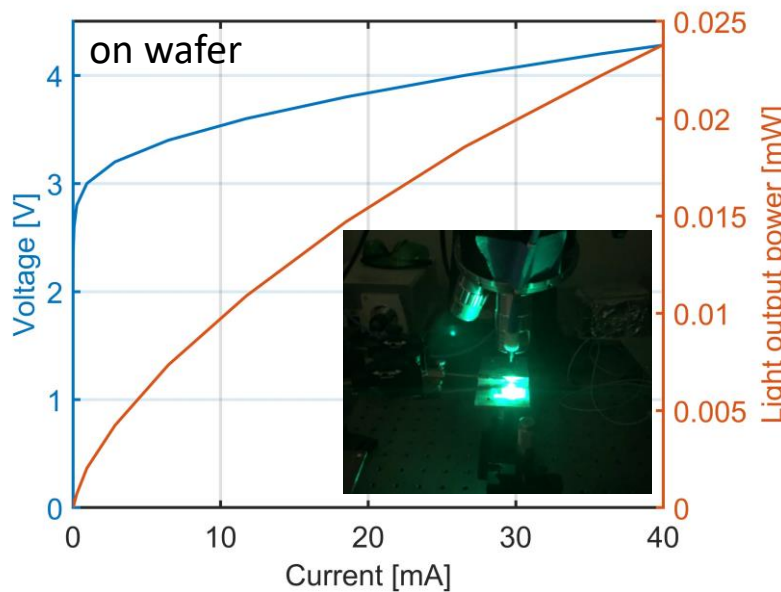
$$Z_{in} = R_s + \frac{R_c(1 + j\omega R_w C_w) + R_w}{(1 + j\omega R_w C_w)(1 + j\omega R_c C_{tot}) + j\omega C_{tot} R_w}$$



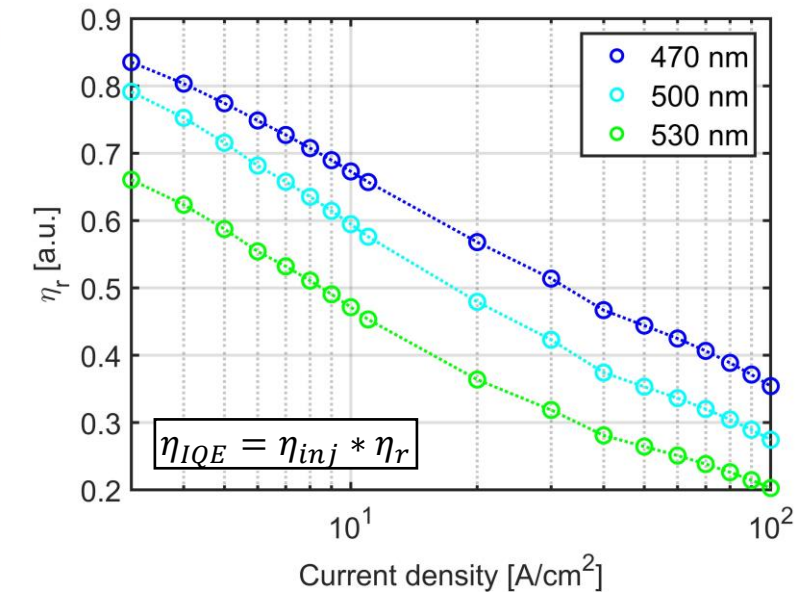
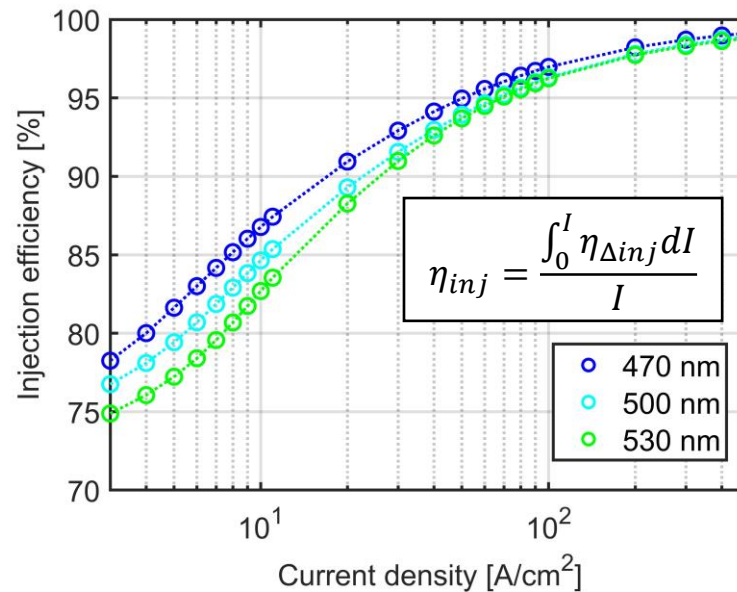
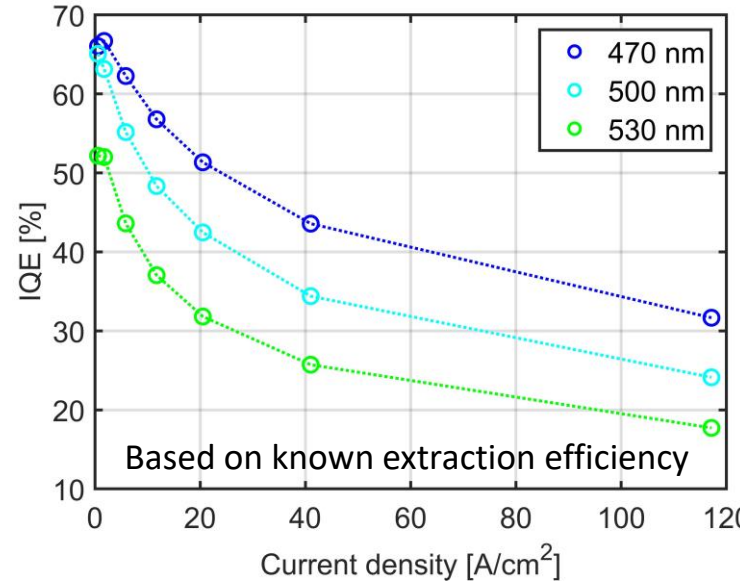
# Wavelength Series on Lumileds Epitaxy

Color	Description
Blue	3 QWs, 3 nm, wavelength 470 nm
Cyan	3 QWs, 3 nm, wavelength 500 nm
Green	3 QWs, 3 nm, wavelength 530 nm

\*LED mesa diameter = 100  $\mu\text{m}$

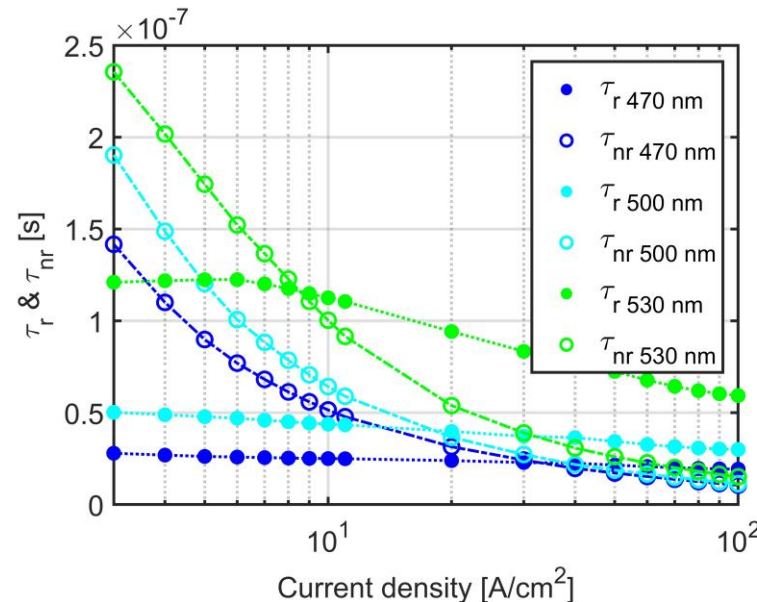
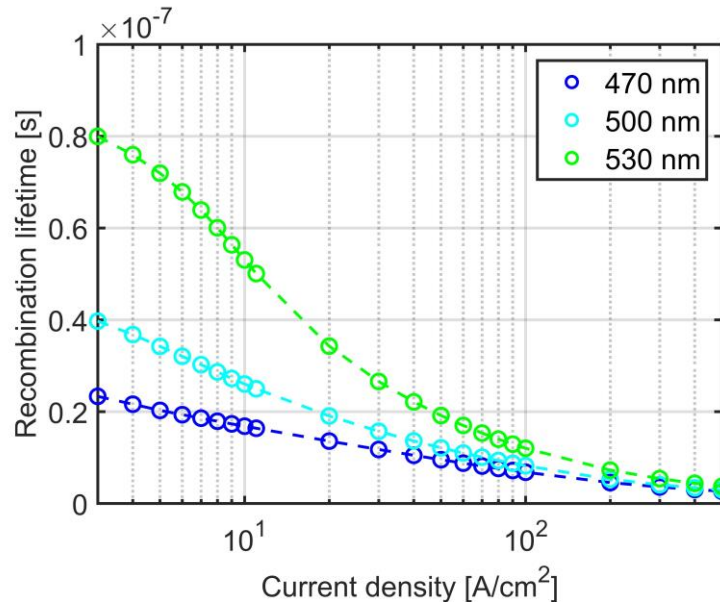


# Internal Quantum, Injection, and Radiative Efficiency



- Longer wavelength → lower IQE, lower injection efficiency, and lower radiative efficiency
- *How much of the change in efficiency from blue to green is due to intrinsic effects (e.g., wavefunction overlap and phase-space filling) vs. extrinsic effects (e.g., material degradation)?*

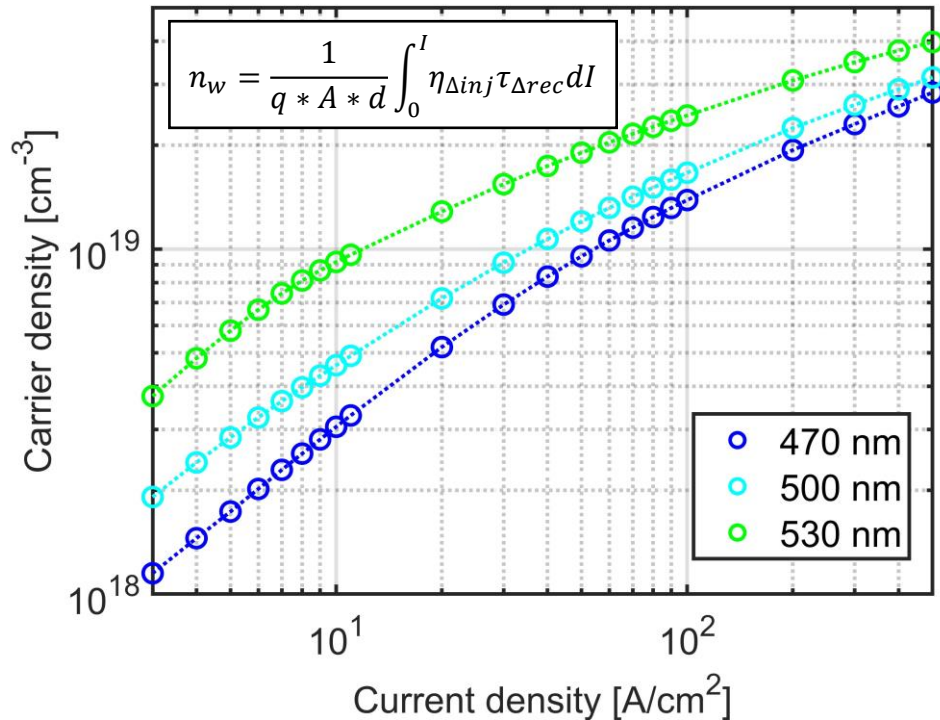
# Radiative and Non-Radiative Lifetimes



$$\eta_r = \frac{\tau_{nr}}{\tau_{nr} + \tau_r}$$
$$\tau_{rec} = \frac{\tau_{nr} * \tau_r}{\tau_{nr} + \tau_r}$$

- The total recombination lifetime is obtained by integrating the differential lifetime
- Radiative lifetime and non-radiative lifetime are separated using total lifetime and radiative efficiency
- Longer wavelength  $\rightarrow$  longer total lifetime, longer radiative and non-radiative lifetimes
- ***Longer lifetimes at longer wavelengths expected from smaller wave function overlap***

# Role of Carrier Density vs. Current Density



$$J \propto A(n)n + B(n)n^2 + C(n)n^3$$

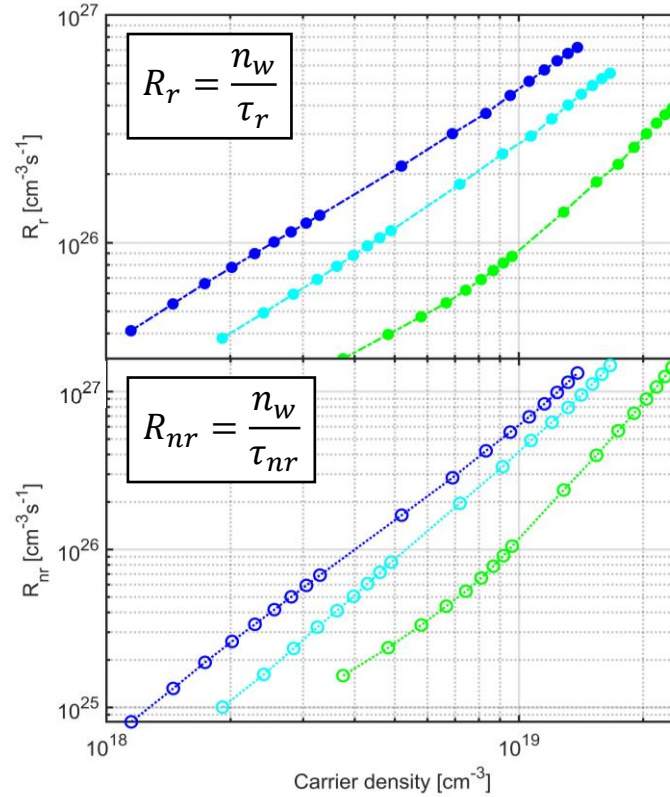
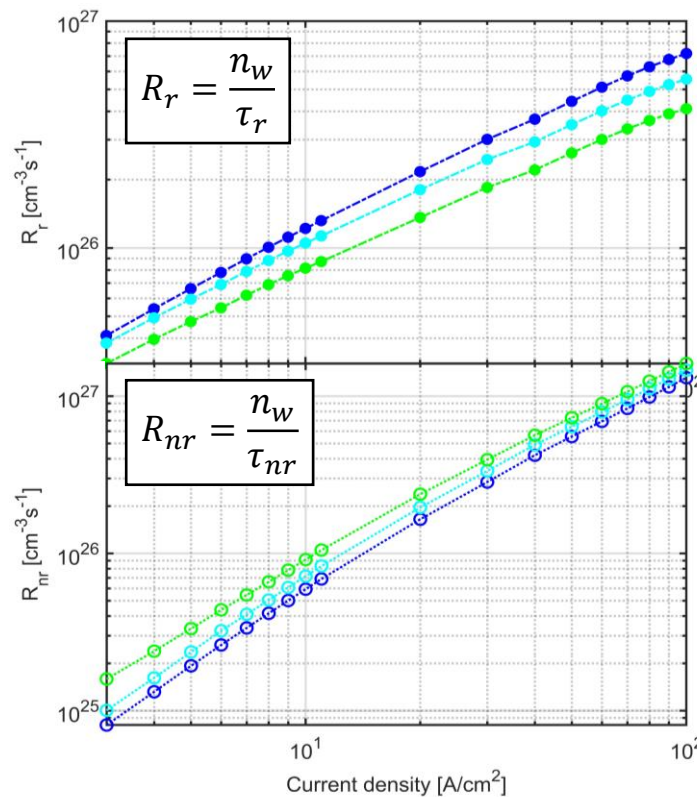
- Longer wavelengths have lower  $A(n)$ ,  $B(n)$ ,  $C(n)$  at a given  $n$  due to stronger QCSE
- Reduces efficiency of converting carriers to current
- Longer wavelengths have higher  $n$  at a given  $J$***
- Increases the relative strength of the Auger term***

# Radiative and Non-Radiative Recombination Rates



$$R_{rec} = \int_0^{n_w} \frac{dn_w}{\tau_{\Delta rec}}$$

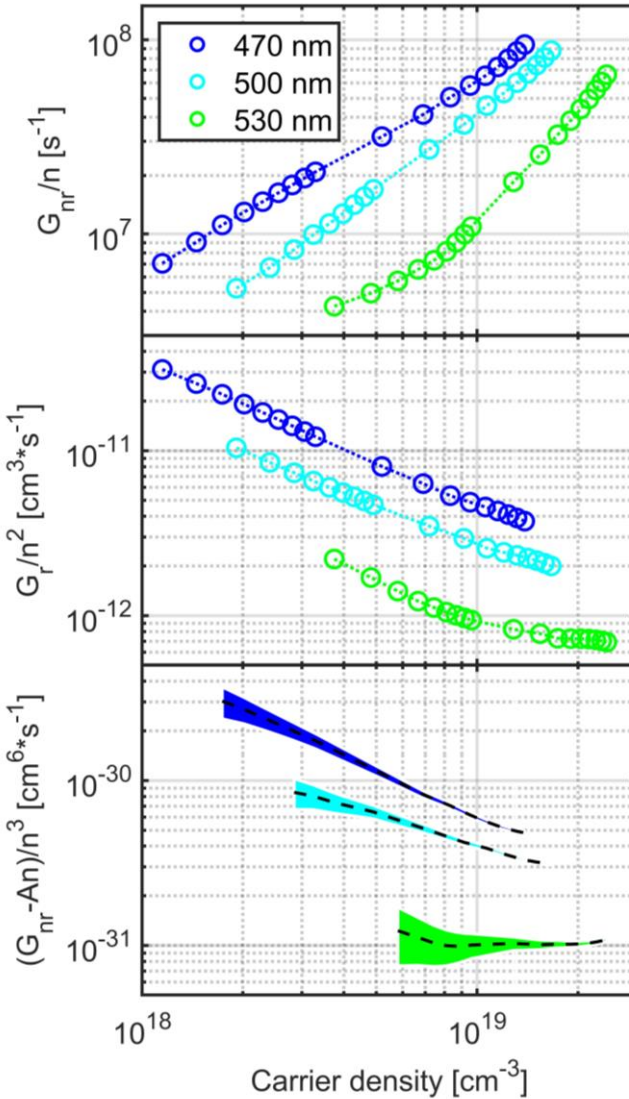
$$\tau_{rec} = \frac{n_w}{R_{rec}}$$



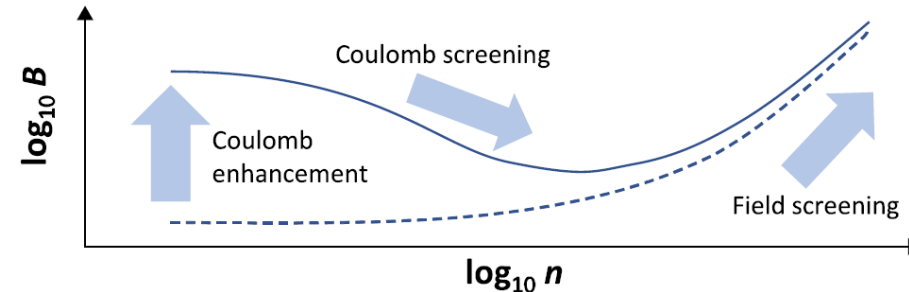
- Longer wavelength  $\rightarrow$  stronger polarization in QWs  $\rightarrow$  lower wave function overlap  $\rightarrow$  smaller  $A$ ,  $B$ , and  $C^*$
- At longer wavelength,  $n$  is higher, but  $B$  and  $C$  are lower
- $R_{nr}(530 \text{ nm}) > R_{nr}(470 \text{ nm})$  but  $R_r(530 \text{ nm}) < R_r(470 \text{ nm})$  since  $R_r \propto n^2$ , while  $R_{nr} \propto n^3$
- *In addition to increased Auger, reduction in radiative rate is an important factor for green gap*

\*E. Kioupakis et al., *Appl. Phys. Lett.*, **101**.23 (2012): 231107.

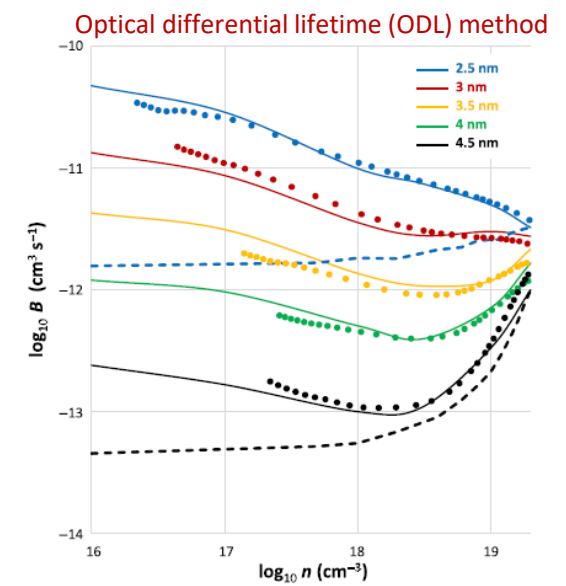
# ABC Parameters



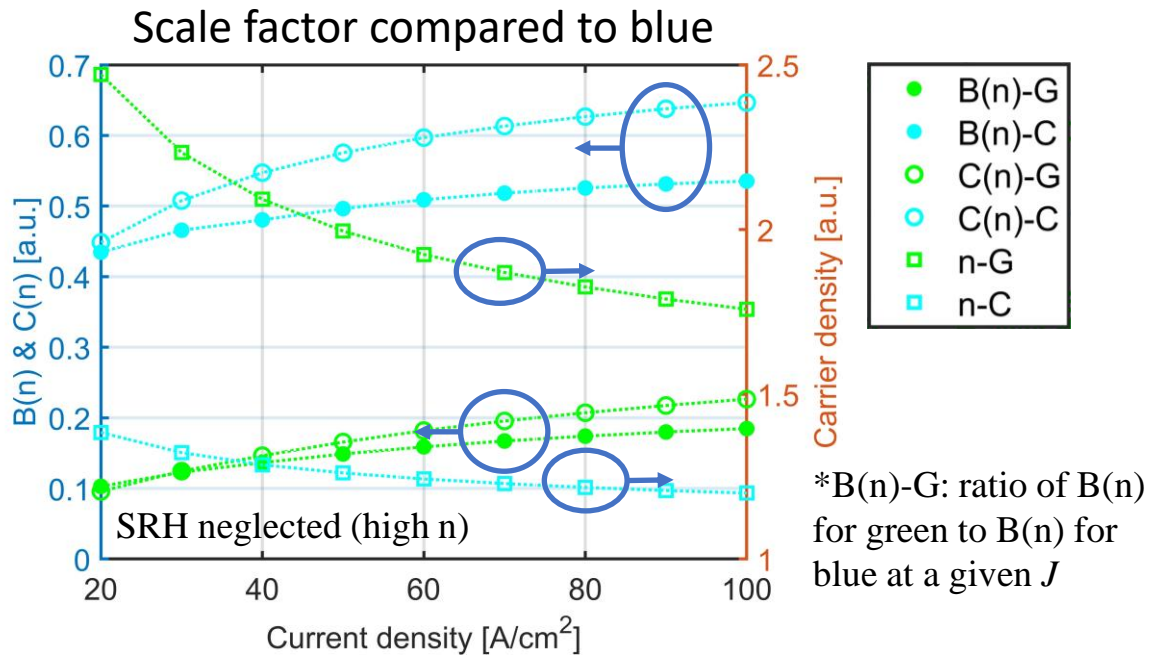
- Mechanisms that affect  $A(n)$ ,  $B(n)$ , and  $C(n)$ : QCSE (field screening), phase-space filling (PSF), and Coulomb enhancement/screening
- $G_{nr}/n$  doesn't converge at low  $n$ , so can only bracket  $A(n)$
- Increase of  $G_r/n^2$  and  $(G_{nr} - An)/n^3$  at low  $n$  attributed to Coulomb enhancement
- Strong field screening not observed in these 3-nm-thick QWs
- Difficult to decouple the different effects but *ratios can provide insight*



A. David et al., *Phys. Rev. Appl.*, 12.4 (2019): 044059.



# $n$ , $B(n)$ , and $C(n)$ Compared to Blue at $40 \text{ A/cm}^2$



## Definition of $B(n)$ & $C(n)$

$$R_r = B(n) * n^2$$

$$R_{nr} \approx C(n) * n^3 \quad (\text{at high } n)$$

Normalized to blue:

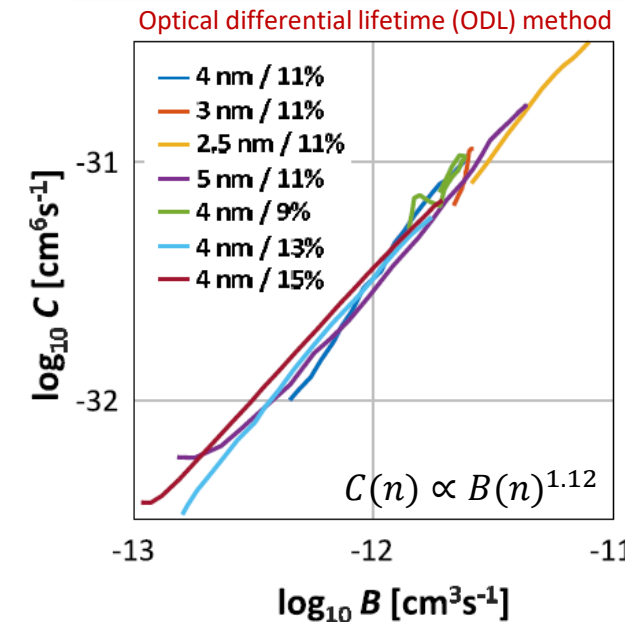
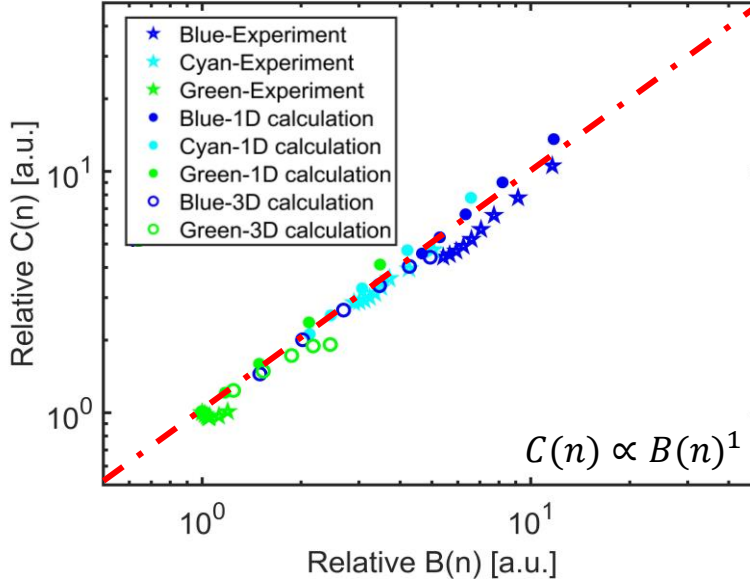
	$R_r$	$R_{nr}$	$n$	$B(n)$	$C(n)$
Blue	1	1	1	1	1
Cyan	0.80	1.16	1.29	0.48	0.55
Green	0.60	1.34	2.09	0.14	0.15

$$\eta_r \approx \frac{B(n)n^2}{B(n)n^2 + C(n)n^3} \quad (\text{at high } n)$$

- Blue  $\rightarrow$  Green:  $R_r$  decreases but  $R_{nr}$  increases
- Blue  $\rightarrow$  Green: Carrier density increases by 2X
- Blue  $\rightarrow$  Green:  $B(n)$  and  $C(n)$  both decrease by 7X
- Efficiency reduction for high  $n$  in longer wavelength LEDs not dominated by large relative increase in  $C(n)$  compared to  $B(n)$***

# Scaling Law Between $C(n)$ & $B(n)$ at High $n$

Simulations by N. Pant and E. Kioupakis, Univ. of Michigan

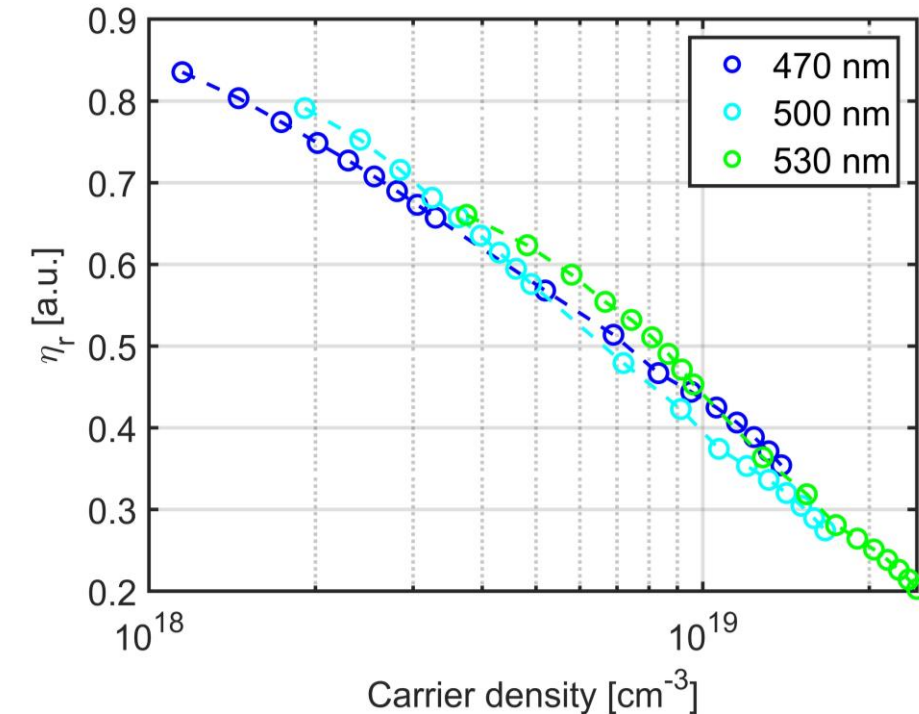
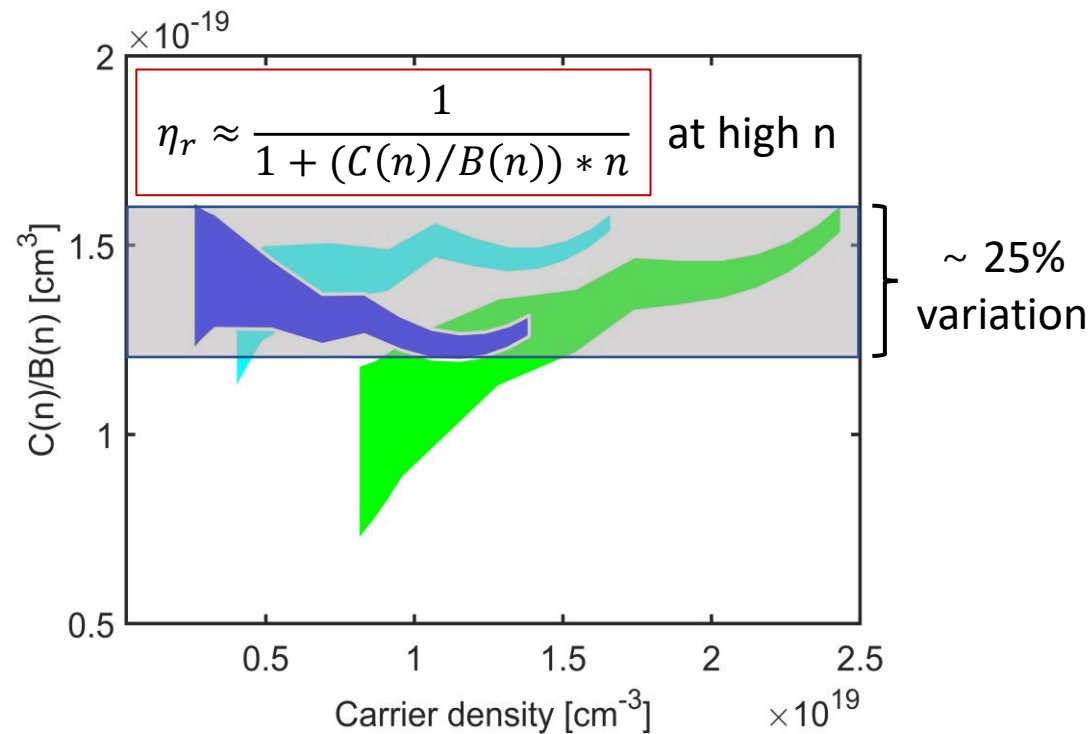


A. David et al., *Appl. Phys. Lett.*, 115.19 (2019): 193502.

- $C(n) \propto B(n)^1$  at high  $n$  from experimental data and Schrödinger-Poisson simulations from Univ. of Michigan
- Simulations capture variations in QCSE, PSF, and alloy disorder
- Same power law obeyed for all wavelengths at high  $n$  under varied polarization fields and PSF
- ***Variations in  $C(n)$  and  $B(n)$  due to QCSE (field screening) and PSF cancel out at high  $n$  if we consider  $C(n)/B(n)$***
- ***Whatever differences exist in  $C(n)/B(n)$  should mainly capture any material-quality differences***

$$\eta_r \approx \frac{1}{1 + (C(n)/B(n)) * n} \quad \text{at high } n$$

# $C(n)/B(n)$ Approaches Similar Value at High $n$



- $C(n)/B(n)$  approaches a similar value at high  $n$  for all wavelengths  $\Rightarrow$  effects of material degradation are small
- Differences in  $C(n)/B(n)$  between blue, cyan, and green consistent with differences in  $C_{bulk}(n)$  from DFT
- ***Decrease of  $\eta_r$  for longer wavelength is mostly from the increase of corresponding  $n$  at a given  $J$***
- ***Radiative efficiency is similar for a given  $n$  for all wavelengths***
- Target green LED designs that reduce  $n$  (multiple QWs) and increase overlap (thin QWs, semipolar, stepped profiles)

# Growth Quality Series on Lumileds Epitaxy

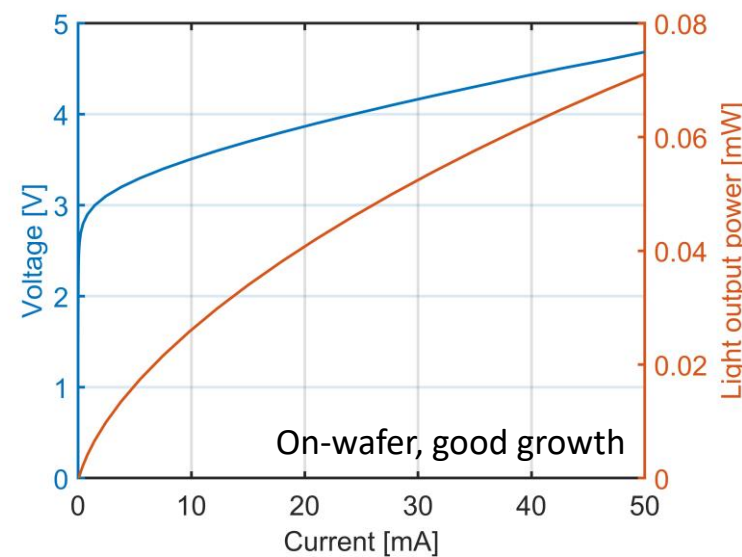


Sample Growth Description	Peak Wavelength @ 2 A/cm <sup>2</sup>	Deep-Level Defect Density [10 <sup>15</sup> cm <sup>-3</sup> ]
Good	534 nm	0.44
Middle	532 nm	0.78
Bad	532 nm	1.50

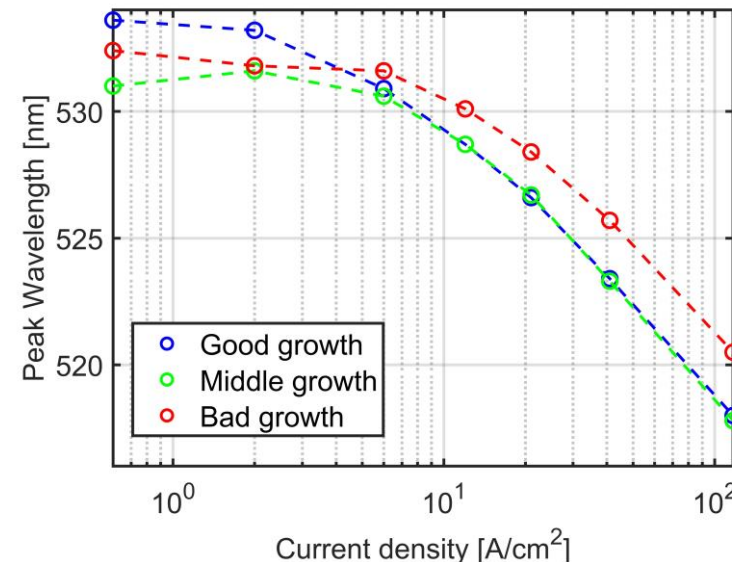
LED mesa diameter = 100  $\mu\text{m}$

Active region: 3 QWs, 3 nm each

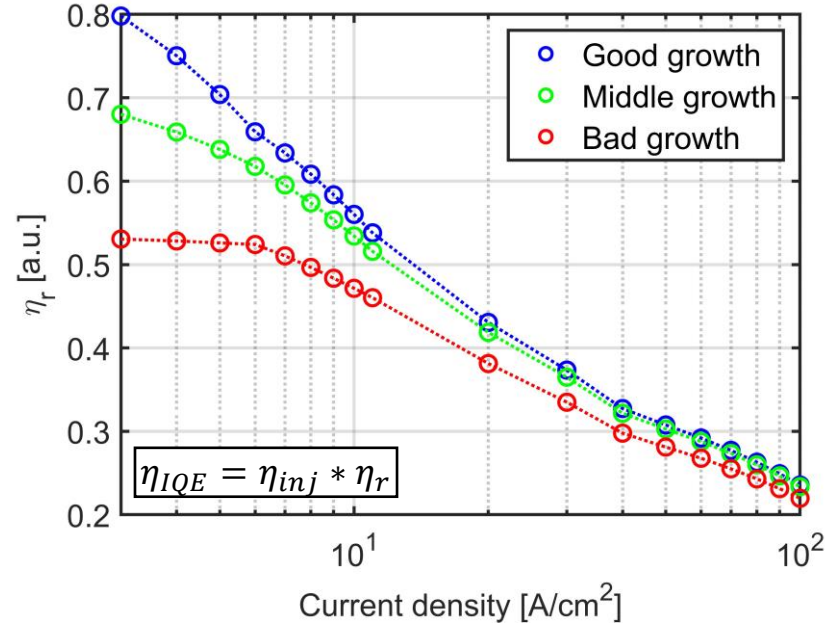
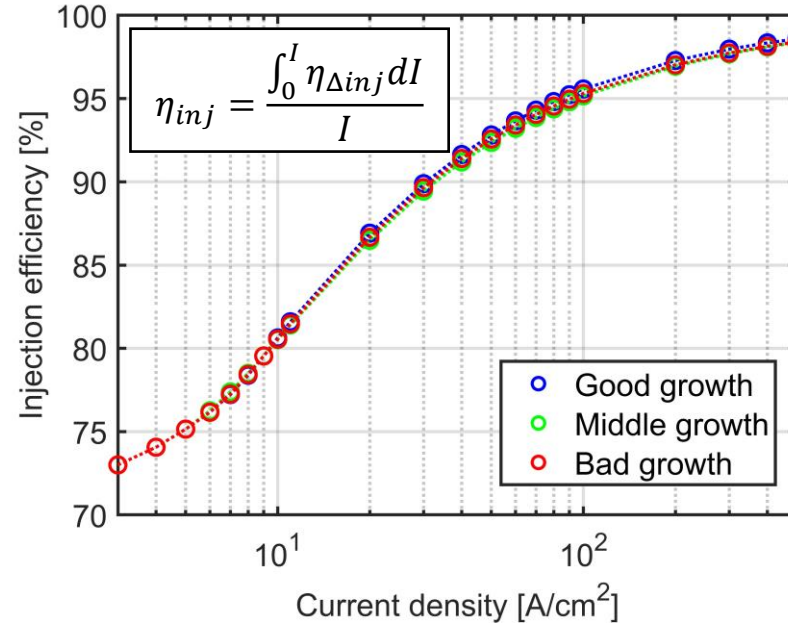
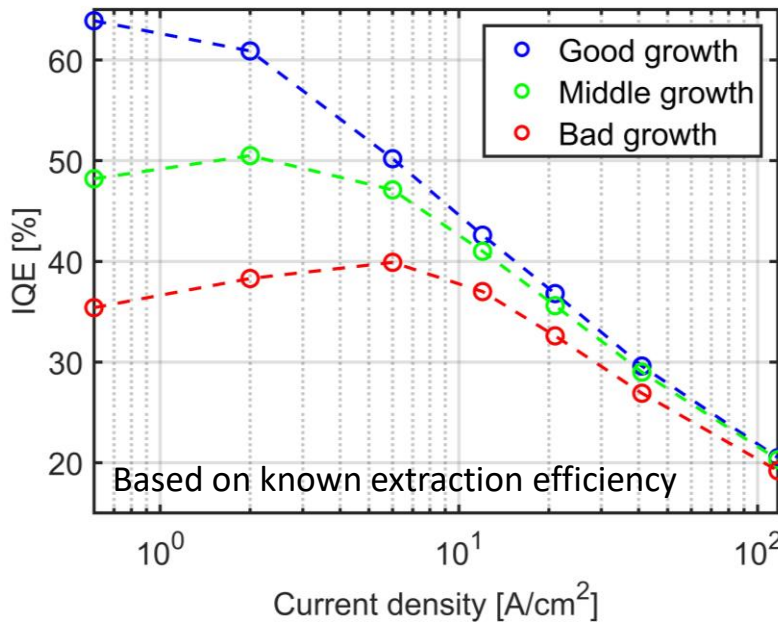
Deep-level defect density ( $N_t$ ) acquired from DLOS



- Study of simplified commercial LED designs
- Representative of recombination behavior in “real” designs
- Design simplification restricts emission to one QW

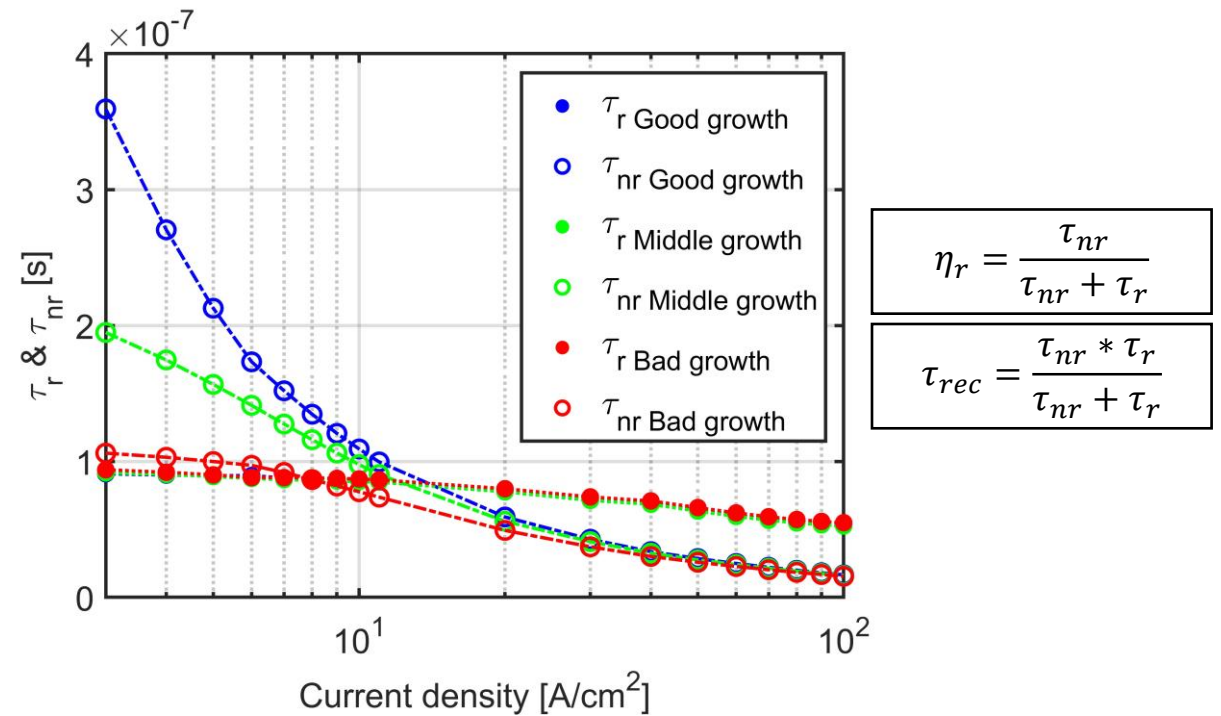
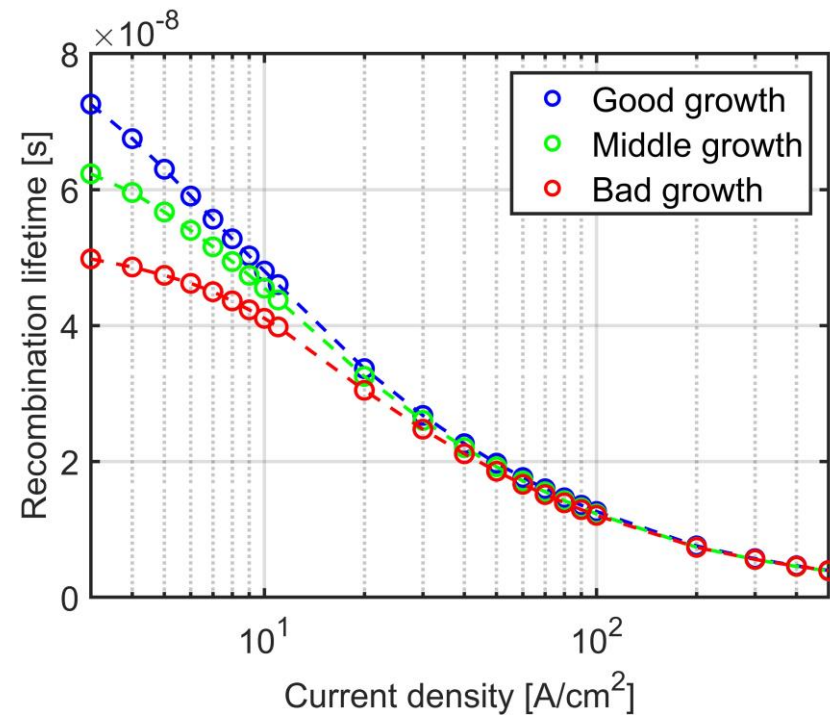


# Internal Quantum, Injection, and Radiative Efficiency



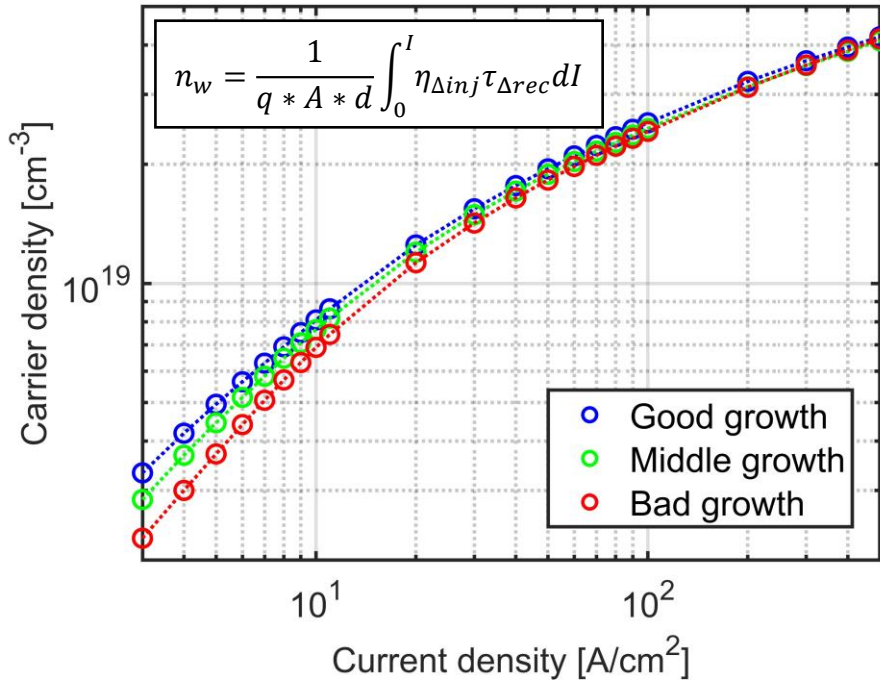
- Lower growth quality is associated with lower IQE at low current (carrier) density
- The three wafers approach a similar value at high current density
- The injection efficiencies are very close for the three wafers
- Lower growth quality has lower radiative efficiency, especially at low  $J$

# Radiative and Non-Radiative Lifetimes



- Lower growth quality has shorter total recombination lifetime ( $\tau_{rec}$ ) at low current density
- Radiative lifetime ( $\tau_r$ ) is similar for all samples
- Non-radiative lifetime ( $\tau_{nr}$ ) only shows large differences at low current density

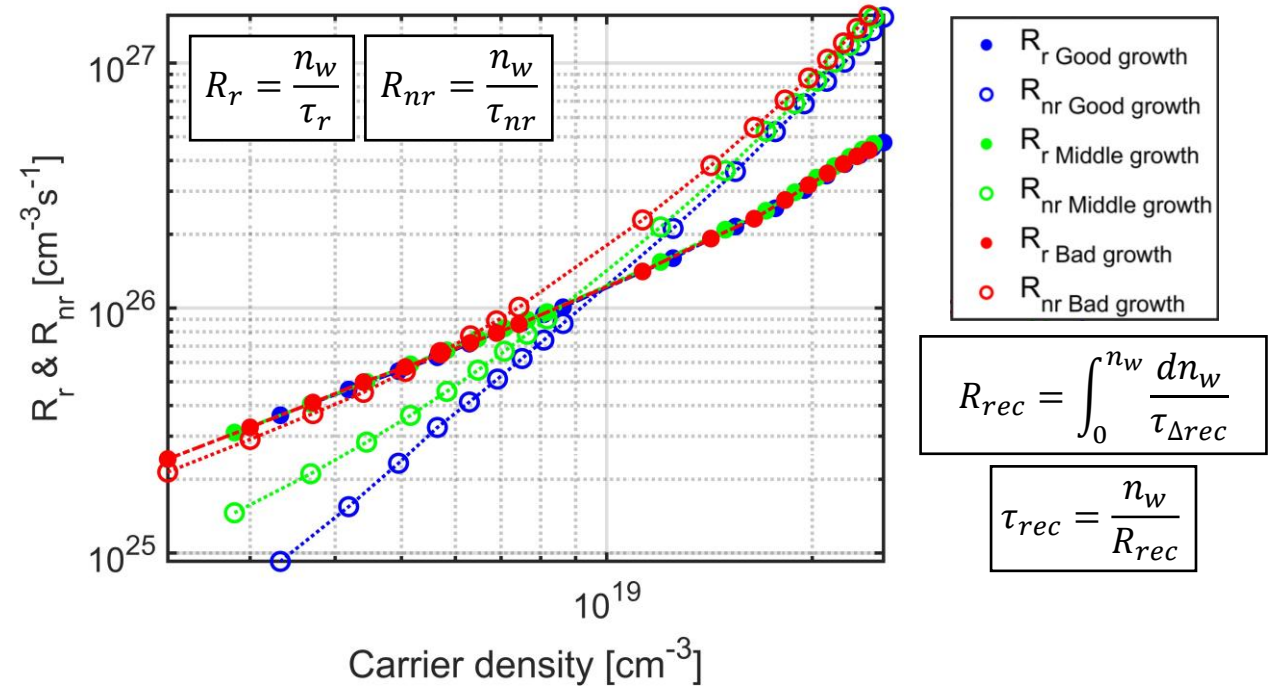
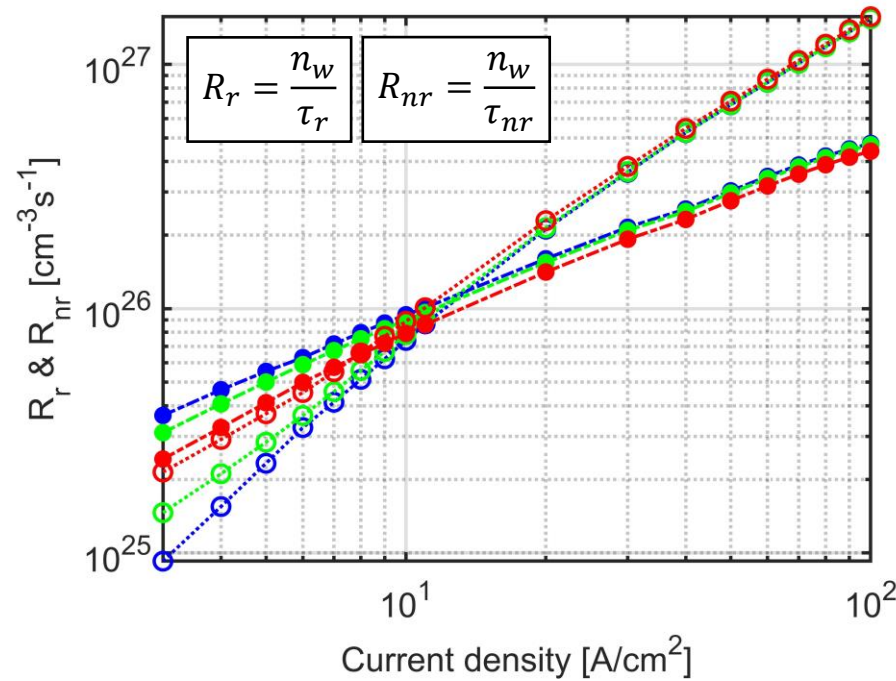
# Carrier Density ( $n$ ) vs. Current Density ( $J$ )



$$J \propto A(n)n + B(n)n^2 + C(n)n^3$$

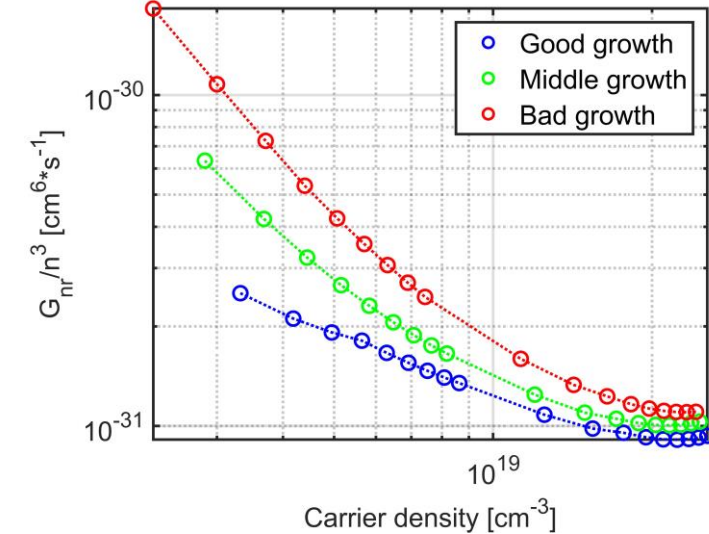
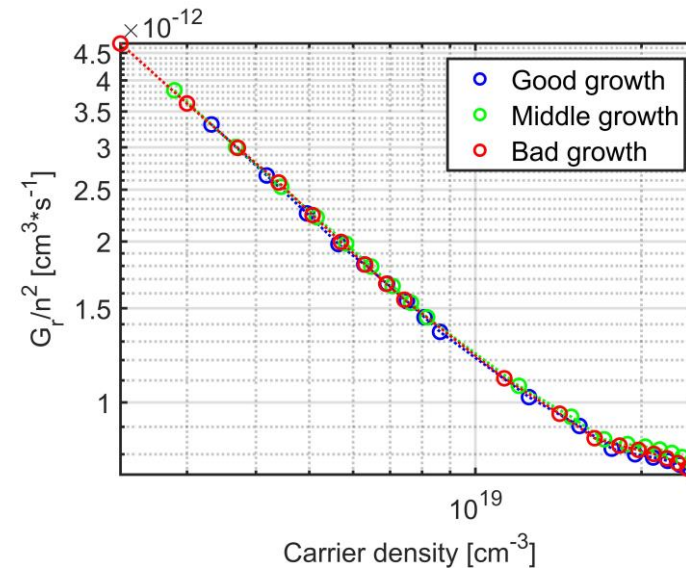
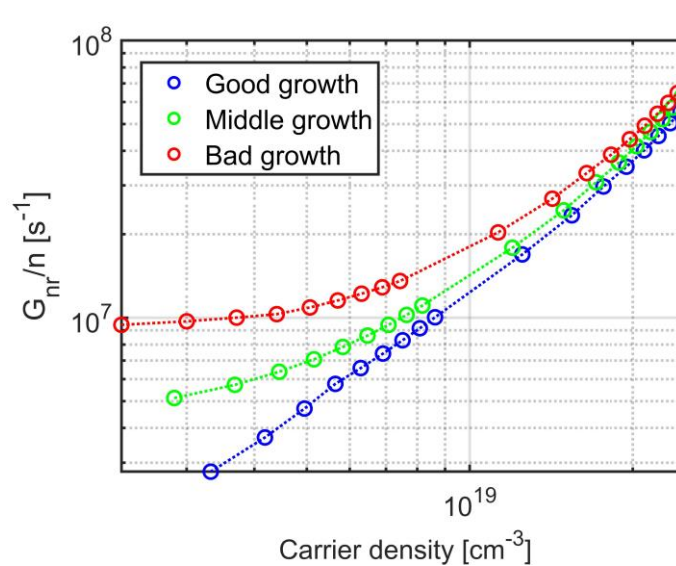
- Larger  $A(n)$  coefficient for lower growth quality is expected
- Lower growth quality has lower carrier density ( $n$ ) at a given current density ( $J$ )
- Differences between samples are most pronounced at low current density

# Radiative and Non-Radiative Recombination Rates



- $R_r$  is similar for the three growth as expected
- $R_{nr}$  is higher for bad growth at low  $n$
- Small change in  $R_{nr}$  at high  $n$  is inconsistent with an  $n^3$  process for TAAR

# ABC Coefficients: $G_{nr}/n$ , $G_r/n^2$ , and $G_{nr}/n^3$

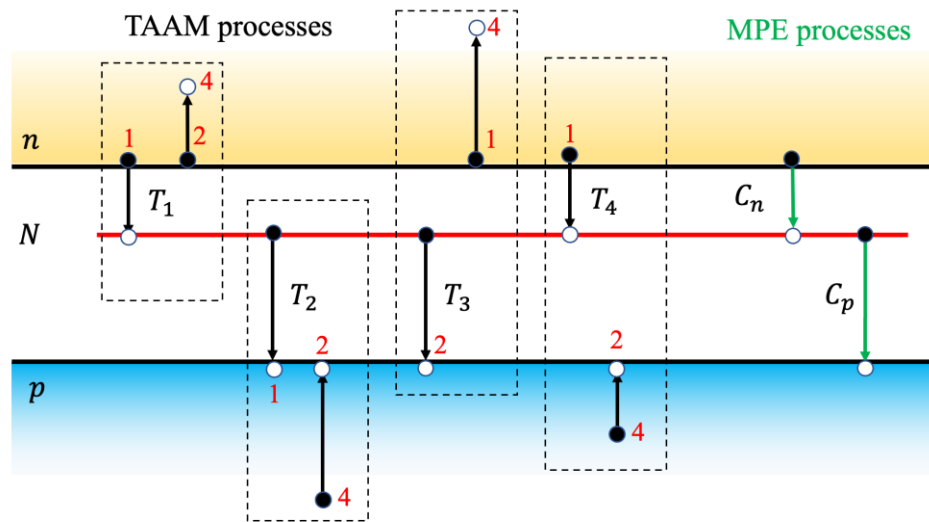


- $A$  can be estimated from  $G_{nr}/n$  using the bad sample at low  $n$
- $B(n) = G_r/n^2$  does not depend on growth quality in the wafers that were studied, as expected
- $G_{nr}/n^3$  depends on growth quality, with higher growth quality having a lower recombination rate

# Trap-Assisted Auger Recombination (TAAR)



Schematic for TAAR (or TAAM) [1]



- TAAR is a form of non-radiative Auger recombination that is assisted by point defects
- The existence of TAAR has been experimentally observed [2,3,4]
- TAAR is suggested as one of the reasons for efficiency decline at high current density
- The carrier density dependence for TAAR has been suggested to be  $n^2$  [1,4] or  $n^3$  [3]
- TAAR is considered to scale linearly with the trap density ( $N_t$ )

1. Zhao, Fangzhou, et al. arXiv preprint arXiv:2211.08642 (2022).
2. Myers, Daniel J., et al. Applied Physics Letters 116.9 (2020): 091102.
3. David, Aurelien, et al. Physical Review Applied 11.3 (2019): 031001.
4. Liu, W., et al. Applied Physics Letters 116.22 (2020): 222106.

# Change in Non-Radiative Recombination

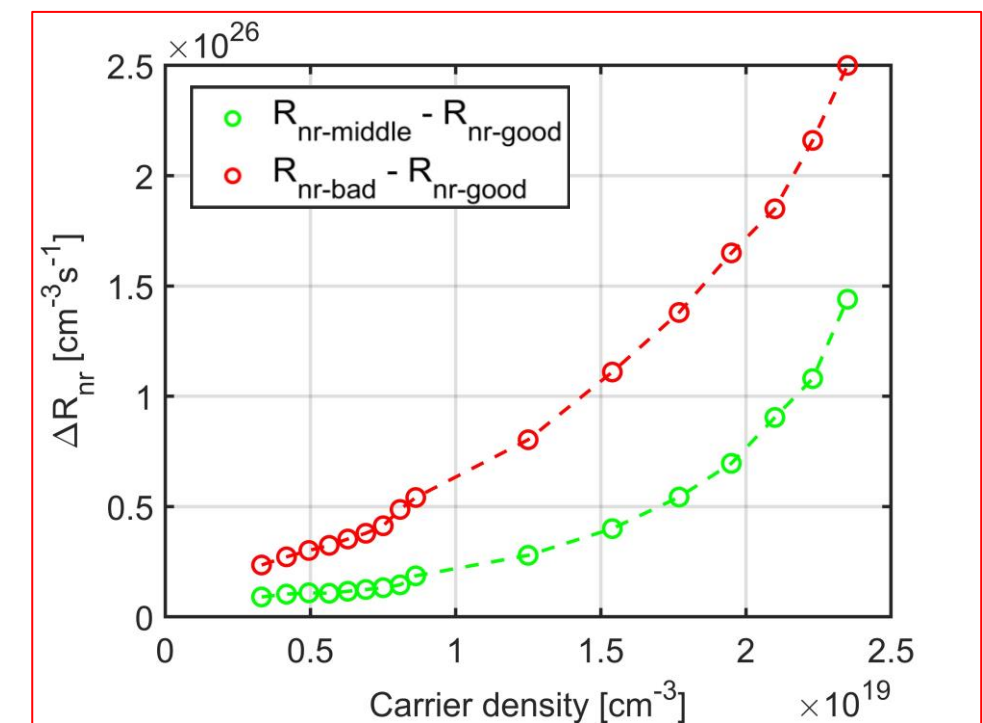
Assuming the recombination rates for SRH and TAAR are proportional to the deep-level defect density ( $N_t$ ) and scales with  $n^2$  [1, 2]

$$R_{nr} = R_{SRH} + R_{Intrinsic\ Auger} + R_{TAAR} = An + C(n)n^3 + Dn^2 = C(n)n^3 + A(n + kn^2) \quad D = k * A$$

Assuming  $R_{Intrinsic\ Auger}$  is independent of  $N_t$

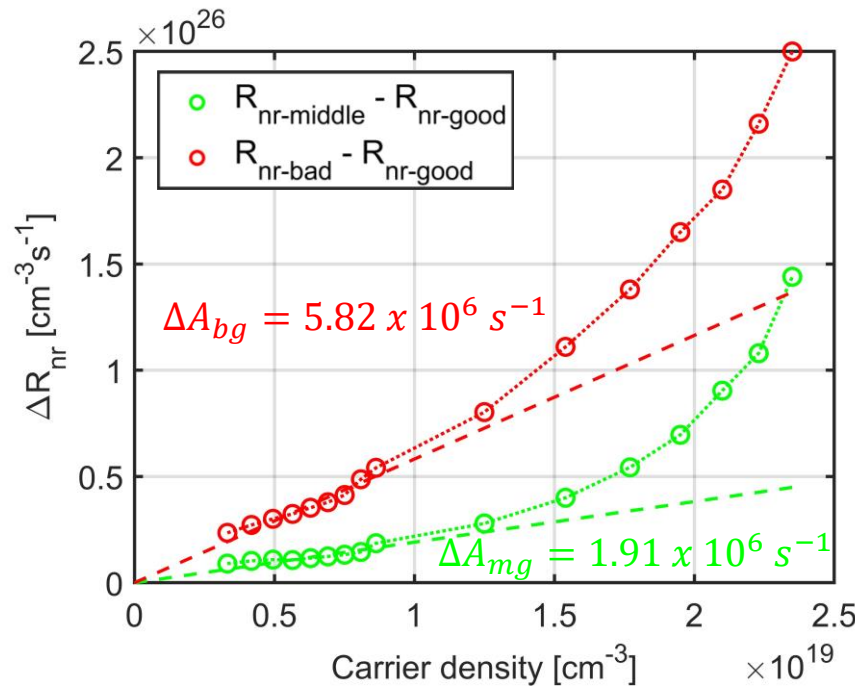
The difference in non-radiative recombination ( $\Delta R_{nr}$ ) for different growth qualities is:

$$\Delta R_{nr} = R_{nr2} - R_{nr1} = \Delta A * n + \Delta D * n^2 = \alpha \Delta N_t (n + k * n^2)$$



1. Espenlaub, Andrew C., et al. Journal of Applied Physics 126.18 (2019): 184502.
2. Zhao, Fangzhou, et al. arXiv preprint arXiv:2211.08642 (2022).

# Change in SRH – Small-Signal vs. DLOS



Deep-level defect density ( $N_t$ ) acquired from DLOS

Growth quality	Good	Middle	Bad
Deep-level defect density [10 <sup>15</sup> cm <sup>-3</sup> ]	0.44	0.78	1.50

From DLOS measurements:

$$\frac{N_{t\_bad} - N_{t\_good}}{N_{t\_middle} - N_{t\_good}} = \frac{1.50 - 0.44}{0.78 - 0.44} \approx 3.12$$

- $\Delta R_{nr}$  is a combination of additional SRH and additional TAAR from decrease in growth quality
- $\Delta A$  can be approximated from the slope of  $\Delta R_{nr}$  at low  $n$  as SRH dominates  $R_{nr}$  ( $\Delta SRH = \Delta A * n$ )

$$\Delta SRH \propto \Delta A \propto \Delta N_t$$

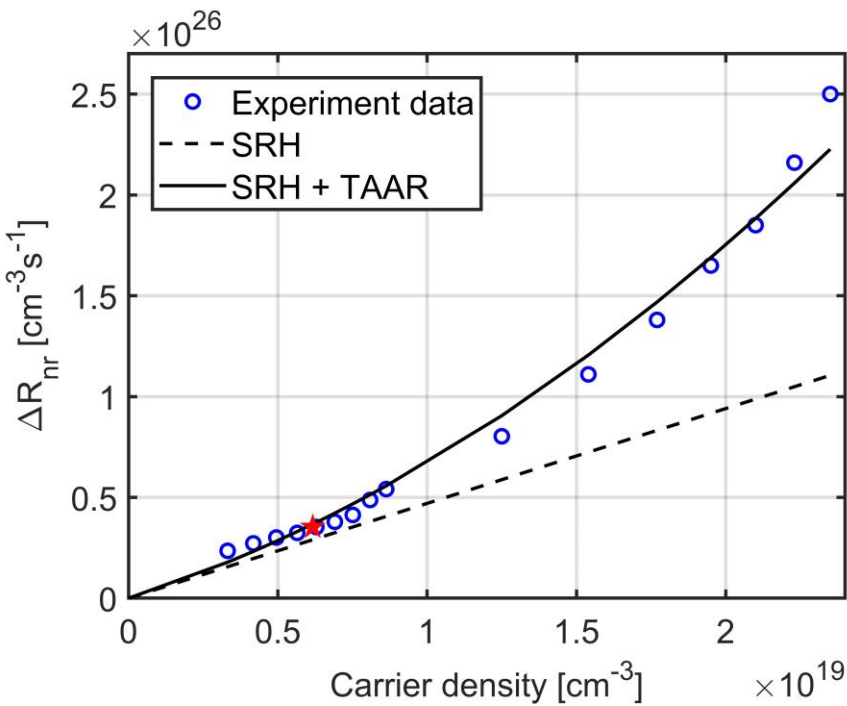
From small-signal carrier dynamics:

$$\frac{\Delta A_{bg}}{\Delta A_{mg}} = \frac{A_{bad} - A_{good}}{A_{middle} - A_{good}} \approx 3.05$$

# Change in TAAR

Fitting of  $\Delta R_{nr}$  between good and bad growth

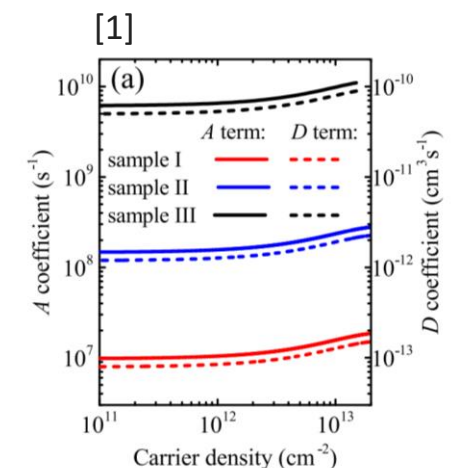
$$\Delta R_{nr} = \alpha \Delta N_t (n + k * n^2)$$



Deep-level defect density ( $N_t$ ) acquired from DLOS and corresponding A and D parameters.

Growth quality	Good	Middle	Bad
Deep-level defect density [ $10^{15} \text{ cm}^{-3}$ ]	0.44	0.78	1.50
$A [\text{s}^{-1}]$	1.95e6	3.46e6	6.65e6
$D [\text{cm}^3 \text{s}^{-1}]$	8.42e-14	1.49e-13	2.87e-13

- For good growth, TAAR  $\sim 10\%$  of  $R_{nr}$ . TAAR would be same order as intrinsic Auger if deep-level defect density increased to  $\sim 10^{16} \text{ cm}^{-3}$ .
- At high  $n$ , SRH follows the same order as TAAR and cannot be ignored, especially in green LEDs.
- TAAR is not a major contributor to efficiency loss in these samples**

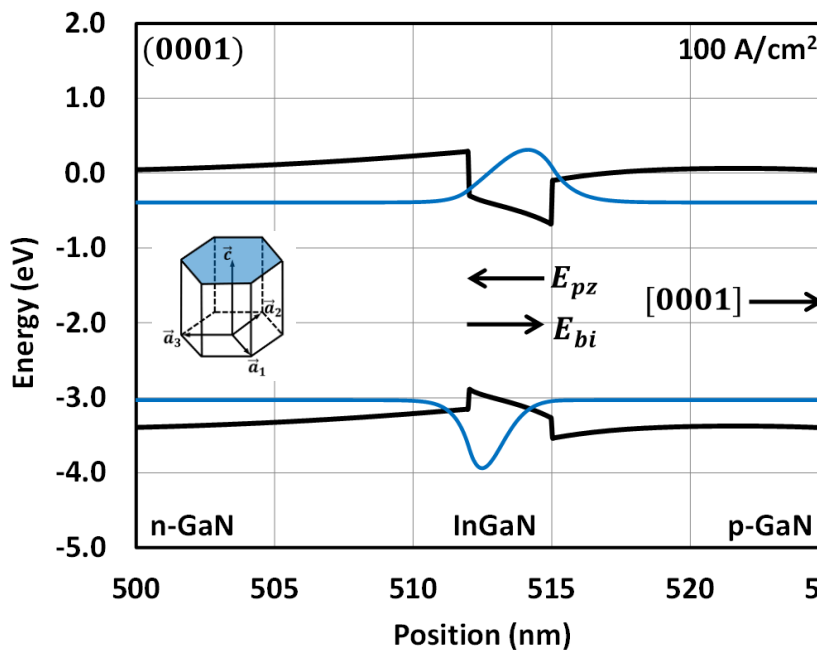


[1] Liu, W., et al. Applied Physics Letters 116.22 (2020): 222106.

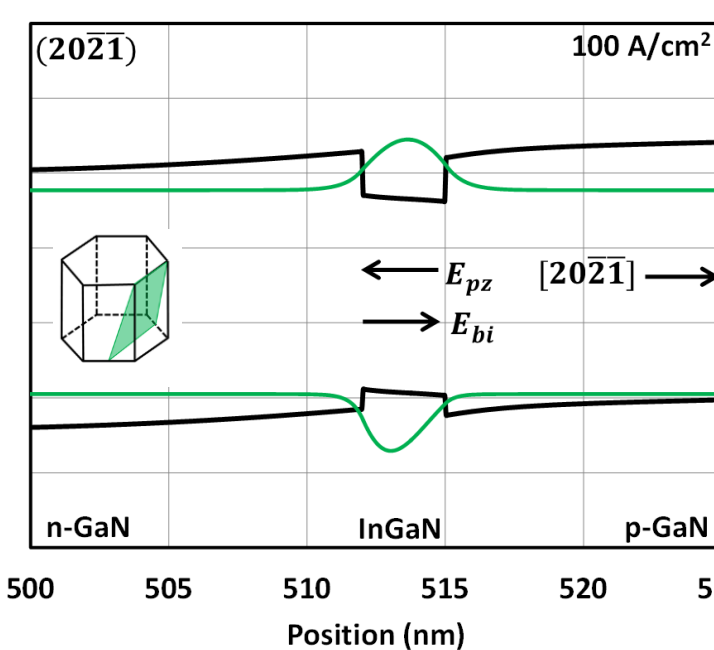
# Orientation Series: Blue LEDs

*Carrier recombination lifetime (rate) influenced by orientation ( $f_{3dB} \propto 1/\tau$ ):*

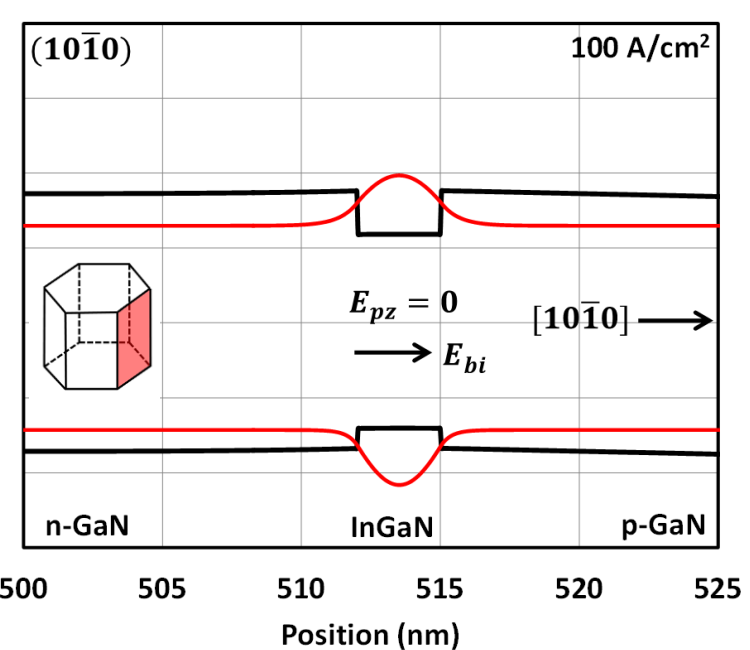
**Polar (0001)**



**Semipolar (2021)**

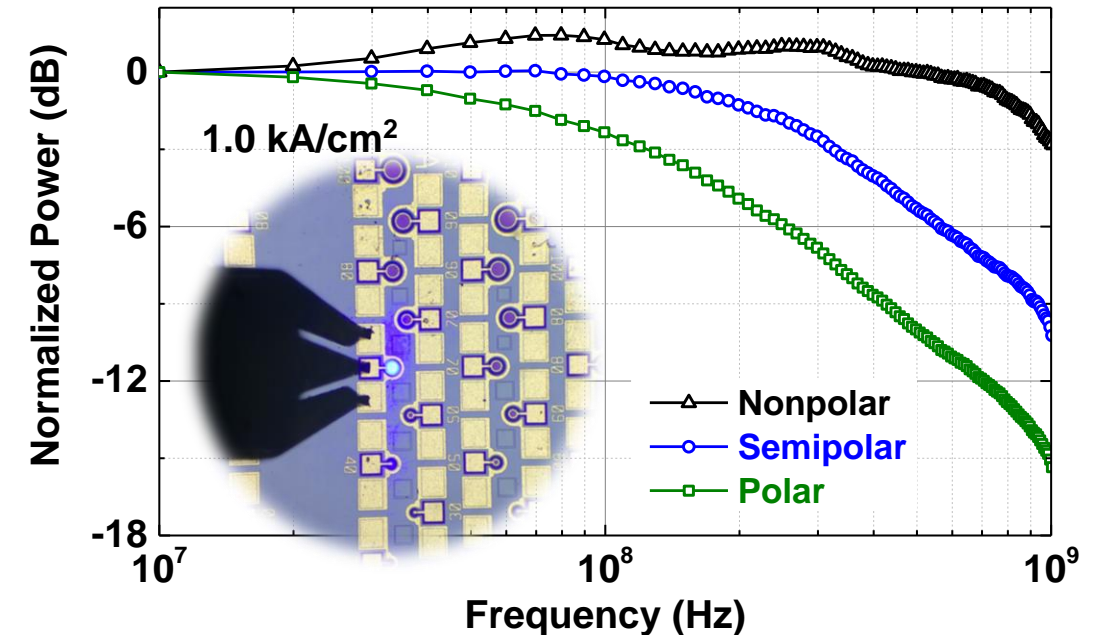
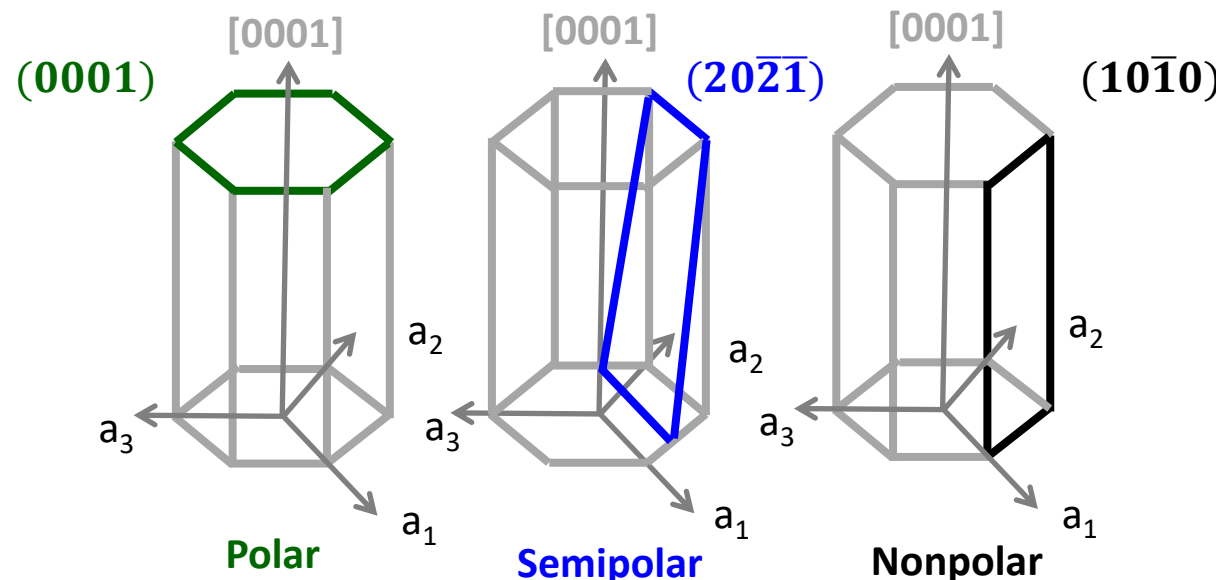


**Nonpolar (1010)**



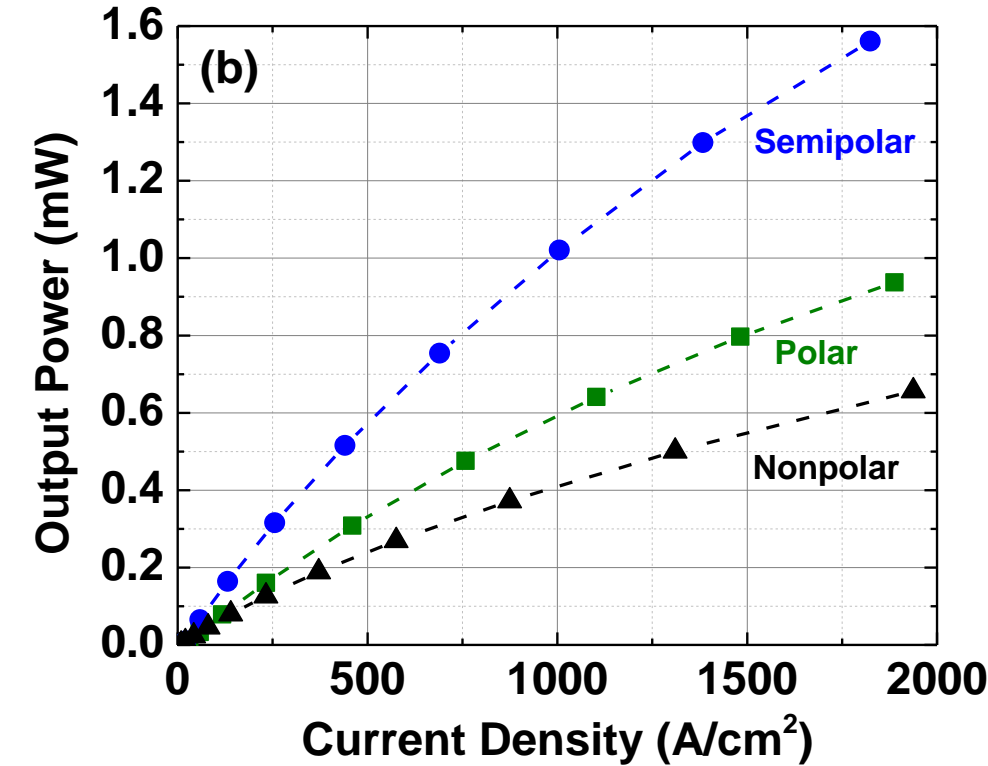
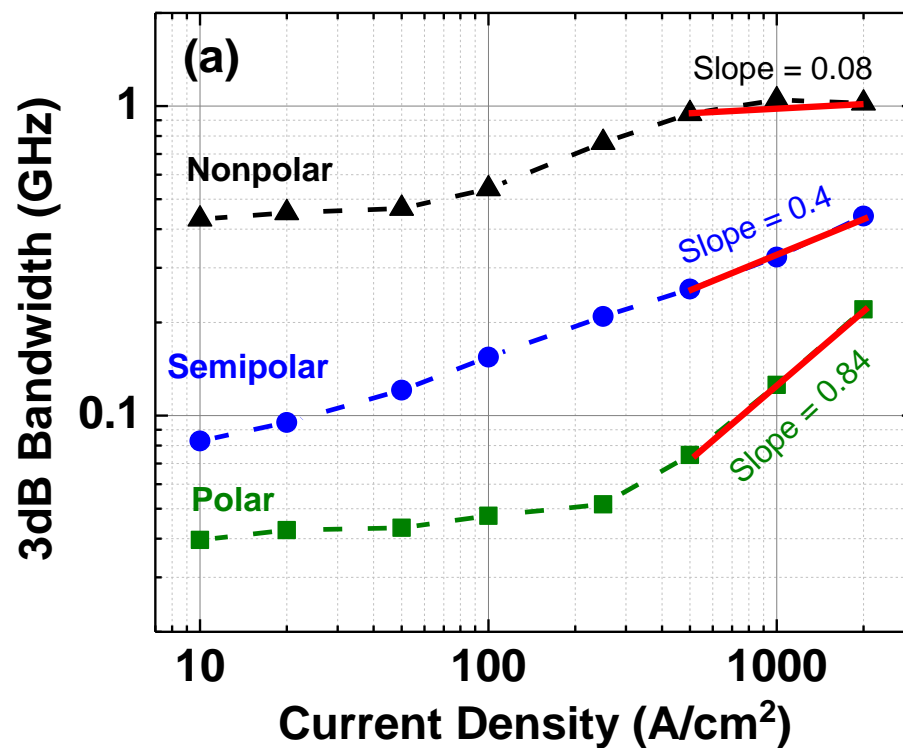
*Goal: Investigate the effects of orientation on modulation bandwidth*

# Orientation Dependence of Bandwidth



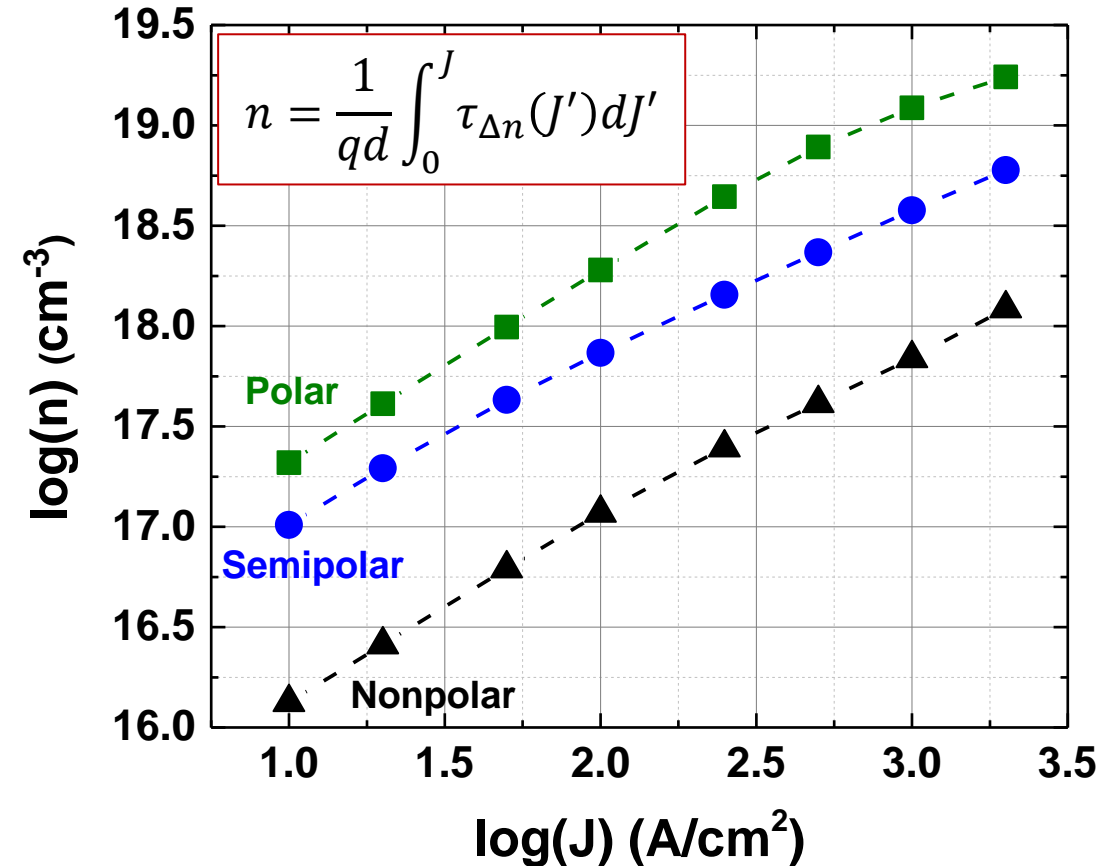
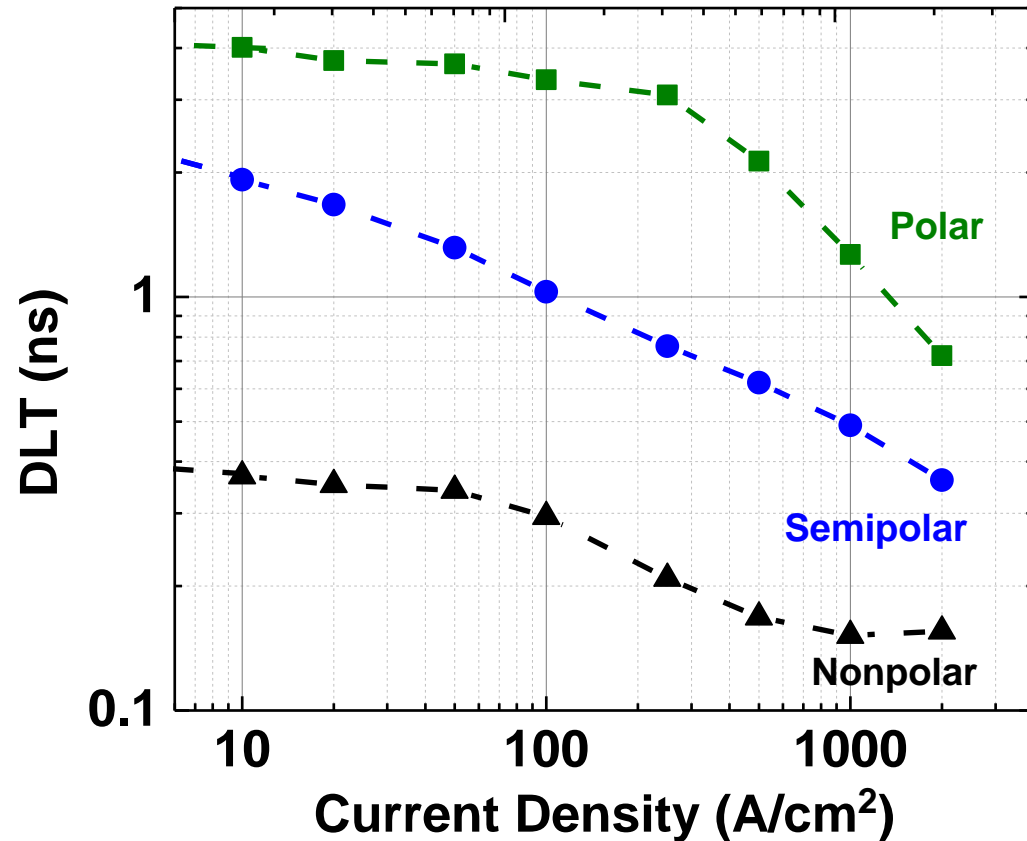
- Compared 450 nm LEDs on polar, semipolar (2021), and nonpolar orientations
- Bandwidth trends follow wavefunction overlap trends
- $f_{3dB\text{-nonpolar}} > f_{3dB\text{-semipolar}} > f_{3dB\text{-polar}}$

# Orientation Dependence of Bandwidth



- Nonpolar and semipolar bandwidth is significantly higher at low current densities
- Polar LED experiences screening of the internal electric fields above  $500 \text{ A}/\text{cm}^2$
- Large bandwidth at low current density important to maximize efficiency

# Differential Carrier Lifetime and Carrier Density



- Differential carrier lifetime (DLT) follows inverse trend to bandwidth
- Carrier density for a given current density always lower on nonpolar and semipolar

# Effect of Wave Function Overlap

- Recombination rate ( $An + Bn^2 + Cn^3$ ) is roughly proportional to the square of the wave function overlap for a given carrier density ( $n$ )
- Overlap is higher in nonpolar/semipolar, increasing the recombination rate and bandwidth
- With higher recombination coefficients ( $A, B, C$ ),  $n$  is lower for a given  $J$
- Lower  $n$  at a given  $J$  reduces the impact of the  $Cn^3$  term

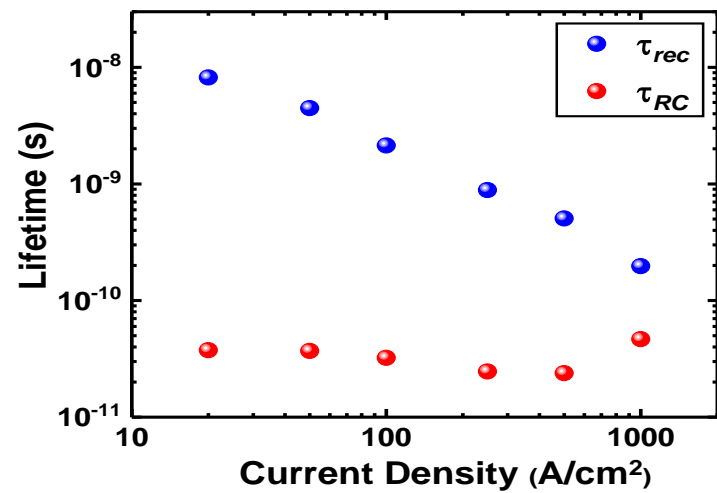
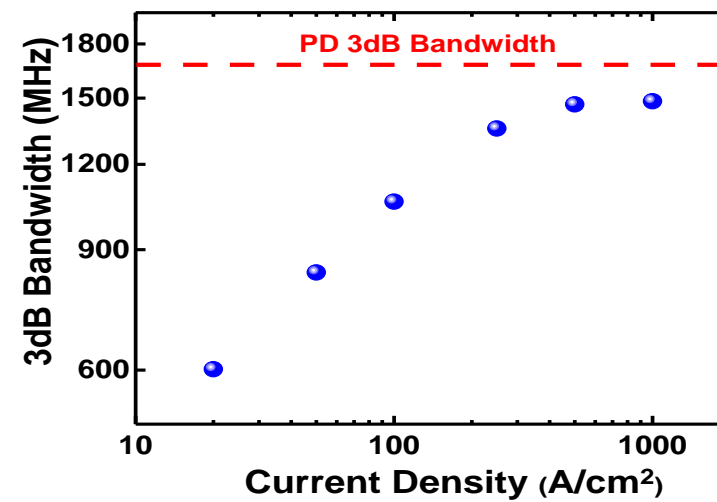
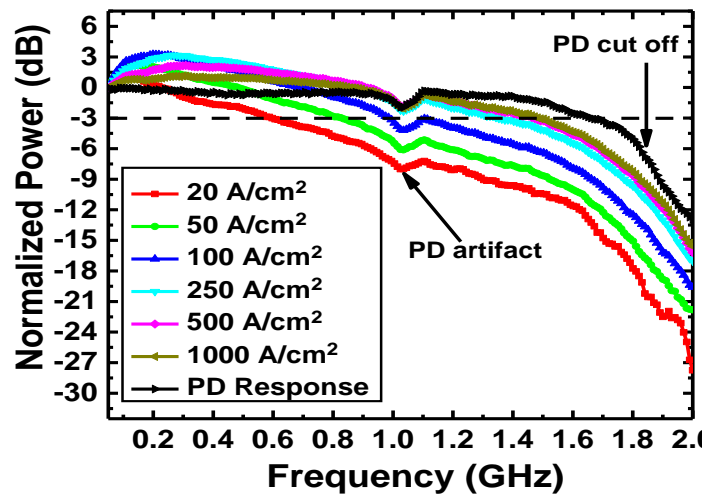
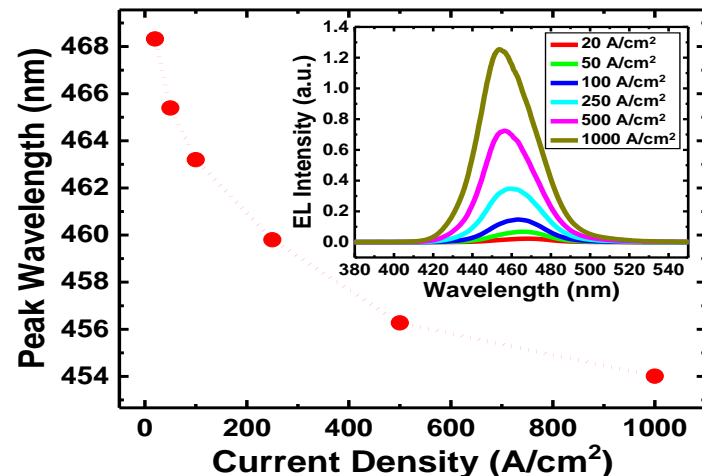
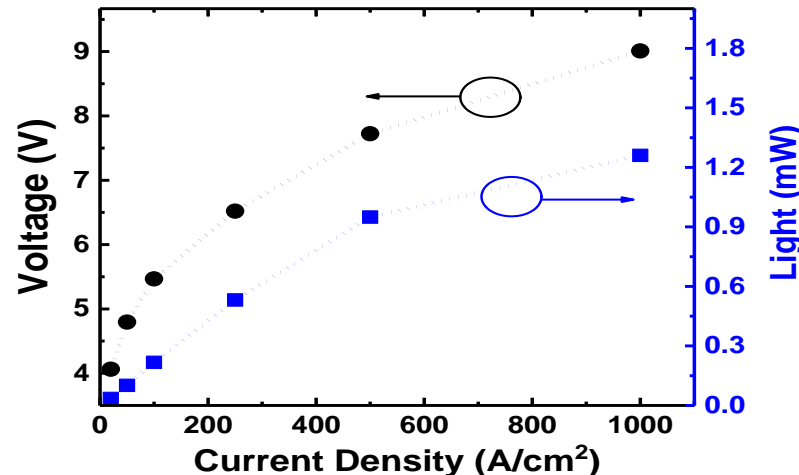
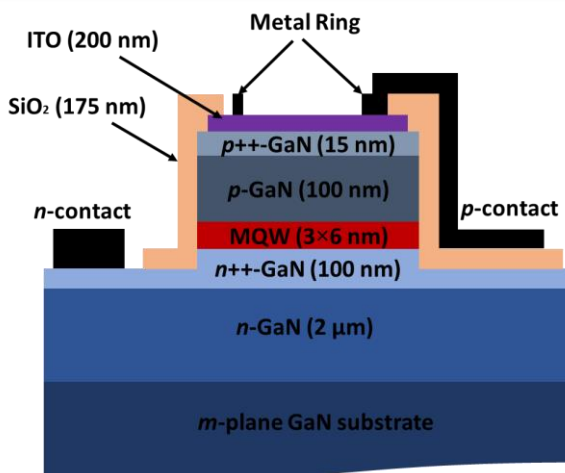
$$A, B, C \propto |\langle F_1 | F_2 \rangle|^2$$

$$J \propto An + Bn^2 + Cn^3$$

$$\eta_r = \frac{Bn^2}{An + Bn^2 + Cn^3}$$

	polar	nonpolar / semipolar
$ \langle F_1   F_2 \rangle ^2$	↓	↑
$A, B, C$	↓	↑
$n$ @ given $J$	↑	↓
$J$ @ given $n$	↓	↑

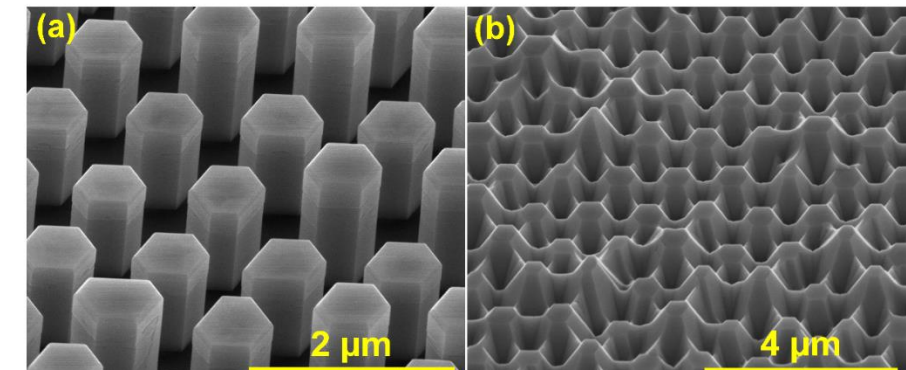
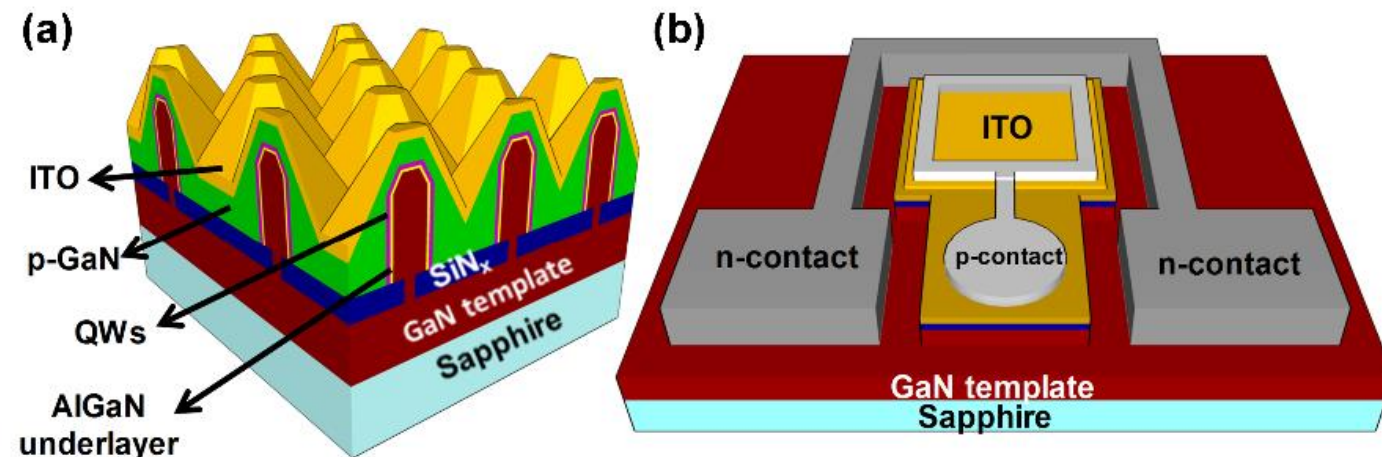
# Nonpolar LED with 1.5 GHz Modulation Bandwidth



*Similar modulation bandwidth to highest reported GaAs-based LED*

A. Rashidi, et al., *Elect. Dev. Lett.* (2018)

# Nonpolar Core-Shell Nanowire-Based LEDs

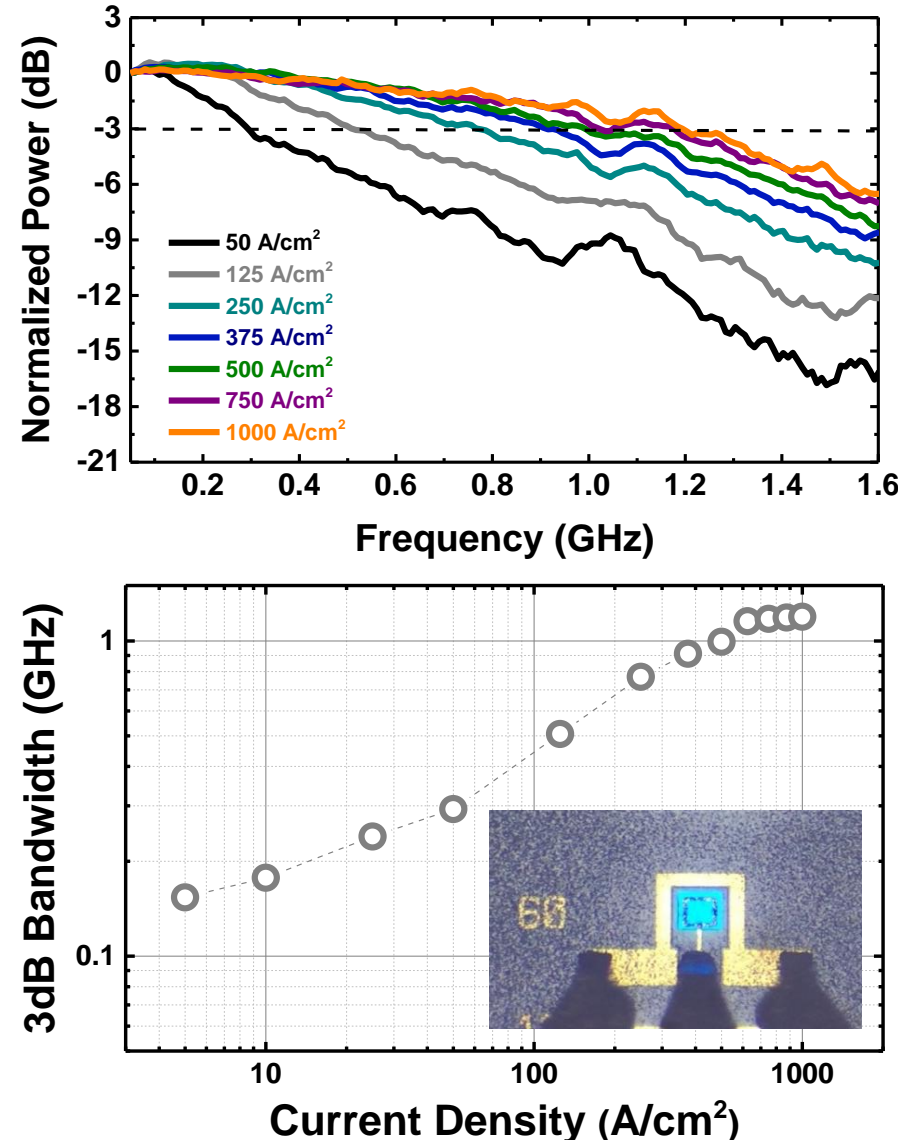


## Potential Advantages:

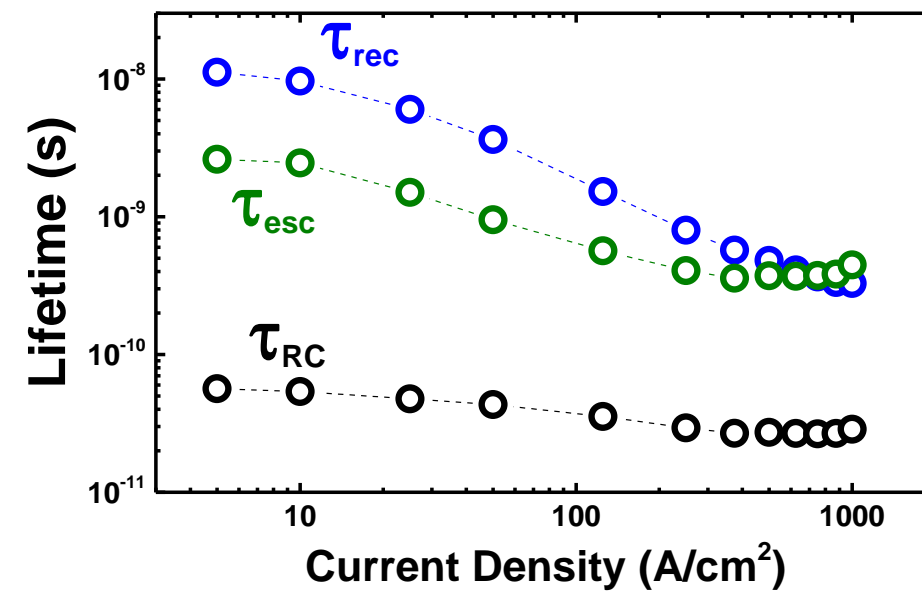
- Polarization-free active regions
- Large effective active region area
- Elimination of threading dislocations
- Strain relaxed structures possible
- Monolithic integration of multi-color LEDs

- Bottom-up selective-area growth
- 4 X 2.5-nm-thick QWs
- $\text{AlGaN}$  underlayer and electron blocking layer
- Peak IQE  $\sim 62\%$
- 60  $\mu\text{m}$  x 60  $\mu\text{m}$  area of NWs

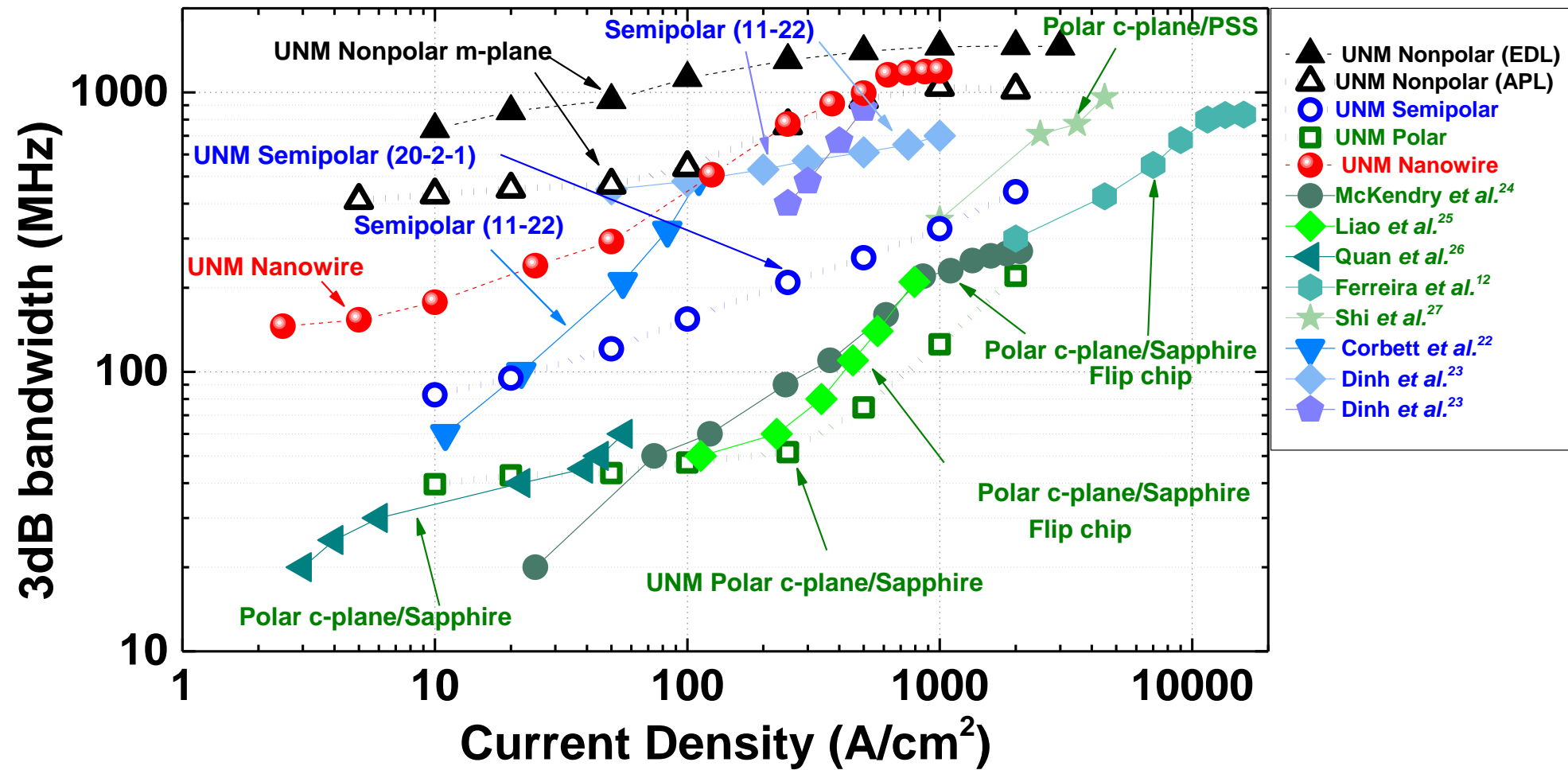
# Frequency Response and Lifetimes



- 1.2 GHz bandwidth at 1 kA/cm<sup>2</sup>
- Non-uniform injection affects spectrum and BW vs. J trend
- *Similar maximum bandwidth to planar m-plane LED*



# Comparison of Bandwidth for Various Orientations



*c-plane bandwidth is fundamentally lower due to internal electric fields (QCSE)*

# Conclusions

---

- Small-signal electroluminescence measurements used to study carrier dynamics in polar, semipolar, and nonpolar LEDs under real operating conditions
- Analysis of an LED wavelength series on commercial epitaxy shows decrease in IQE for longer wavelength is mostly from the increase of corresponding  $n$  at a given  $J$
- Analysis of a green LED growth quality series on commercial epitaxy shows TAAR is not a major contributor to efficiency loss
- Nonpolar and semipolar orientations are fundamentally faster than  $c$ -plane, as expected from increased wave function overlap
- Core-shell nanowire LEDs showed  $>1$  GHz 3dB bandwidth

Thank You!



SNL is managed and operated by NTESS under DOE NNSA contract DE-NA0003525